Unraveling viral identity: Avoiding the trap of endogenous sequences for viral surveillance of small ruminant oncogenic retroviruses

Riocreux-Verney Benjamin[1], Verneret Marie[1,2], Dolmazon Christine[1], Shirin Ashraf[3], Stella A. Atim[3,4,5], Navratil Vincent [6,7], Leroux Caroline[1 ¶,*], Turpin Jocelyn[1 ¶,*]

[1] IVPC UMR754, INRAE, Universite Claude Bernard Lyon 1, EPHE, Université PSL, France.

[2] Universite Claude Bernard Lyon 1, LBBE, UMR 5558, CNRS, VetAgro Sup, Villeurbanne, France.

[3] MRC-University of Glasgow Centre for Virus Research, (CVR), Glasgow, UK.

[4] MRC/UVRI and LSHTM Uganda Research Unit, Entebbe, Uganda.

[5] Ministry of Agriculture, Animal Industry and Fisheries, Entebbe, Uganda

[6] PRABI, Pôle Rhône-Alpes Bioinformatics Center, Universite Claude Bernard Lyon 1, Villeurbanne, France.

[7] European Virus Bioinformatics Center, Leutragraben 1, Jena, Germany.

*Correspondence: caroline.leroux@inrae.fr and jocelyn.turpin@inrae.fr

¶These authors contributed equally to this work and share last authorship.

Keywords

Virome, endogenous retrovirus, vectors, small ruminants, JSRV, ENTV

Abstract

Small ruminants (sheep and goats) are one of the few mammals in which an exogenous retrovirus (XRV) and closely related endogenous retroviral elements (ERV) coexist within the same host genome. The betaretroviruses Jaagsiekte sheep retrovirus (JSRV) and enzootic nasal tumor virus (ENTV) cause pulmonary and nasal adenocarcinomas, respectively, and share extensive sequence similarity with their endogenous counterparts. Consequently, molecular surveillance must rely on assays that can unequivocally distinguish true exogenous infection from ERV-derived templates; failure to do so compromises diagnosis, phylogenetic inference, and epidemiological conclusions.

We retrieved all complete JSRV, ENTV-1/2, and related ERV genomes deposited in public repositories and performed a comprehensive alignment. Only a limited number of genomic segments were capable of distinguishing exogenous from endogenous sequences. We refer to these as discriminating regions (DRs). Phylogenies built using DRs revealed that several entries annotated as XRV are, in fact, ERV-derived or chimeric artefacts generated by short-amplicon reconstruction.

A systematic literature review of over 100 articles identified 286 distinct primers and probes used for the XRV amplification. *In-silico* mapping of each oligonucleotide onto the full alignment showed that only 28 % reliably differentiate XRV from ERV. We experimentally validated the predictive power of this approach for 17 primer/probe sets, confirming that non-discriminating assays produce false-positive signals from endogenous templates.

The misannotation of ERV sequences as exogenous viruses has resulting in the population of databases with dubious entries, fostering erroneous hypotheses such as vector-borne transmission of JSRV and ENTV. To address this issue, we propose a concise set of criteria for assay design, validation, and database annotation emphasizing DR targeting, specificity testing against endogenous templates, and transparent reporting.

Although this framework was developed for small ruminants, it is readily applicable to any host–virus system in which exogenous viruses coexist with endogenous viral elements. This will strengthen viral surveillance, phylogenetics, and the One Health initiatives.

Author Summary

Small ruminants host Jaagsiekte sheep retrovirus (JSRV) and enzootic nasal tumor virus (ENTV) together with numerous endogenous retroviral (ERV) sequences integrated into their genomes. This coexistence makes them a system for studying host-virus co-evolution. However, it also poses significant challenge for viral surveillance and sequencing. A systematic review of the literature on the detection and sequencing of these oncogenic retroviruses revealed a recurring methodological flaw: many studies design molecular assays and experimental conditions without taking into account the abundant ERV background. Consequently, samples reported as containing an exogenous virus often represent artificial chimeras generated by primer cross-reactivity with ERV sequences, or misidentified endogenous elements that are mistaken for an exogenous infection. This oversight contaminates reference

67 databases, propagates erroneous annotations, and can lead to false conclusions,
68 particularly in metagenomic investigations where it is essential to distinguish
69 endogenous from exogenous retroviral reads. Robust assay design must therefore
70 explicitly discriminate between ERV and exogenous retrovirus sequences. In addition,
71 validation should include controls that confirm the presence of truly infectious
72 retroviruses. The small-ruminant case therefore exemplifies a broader challenge in
73 virology for assuring the accurate detection and monitoring of viral infections in species
74 with endogenous viral repertoires.
75

76 # Introduction

77 Cancers induced by the exogenous retroviruses (XRVs), Jaagsiekte Sheep RetroVirus
78 (JSRV) and Enzootic Nasal Tumor Virus (ENTV), have been documented in all regions
79 where sheep and goats are reared, except in Australia, New Zealand, the Falkland
80 Islands and Iceland, where JSRV has been eradicated [1–3]. Multiple copies of
81 endogenous retrovirus (ERV) family II.5, previously named enJSRV and enENTV
82 [4,5], are present in goats (ERV II.5 Ch for *Capra hircus*) and sheep (ERV II.5 Oa for
83 *Ovis aries*), with an average of 223 and 98 loci respectively [6]. The presence of whole
84 copies with little divergence and with preserved open reading frames (*gag, pro, pol*
85 and *env*), suggests the recent activity of ERV II.5 Ch in goats [6]. Despite their close
86 genetic relationship with domestic sheep and goats XRVs, ERVs are not implicated in
87 the development of respiratory cancers in domestic small ruminants. Therefore, the
88 exogenous retroviruses JSRV and ENTV remain the only known aetiological agents
89 of respiratory cancers in domestic small ruminants.

90 Developing robust virus detection tools is an essential for managing the infectious risk
91 posed by these incurable, fatal and transmissible cancers that threaten small-ruminant
92 farming. Serological detection of antibodies is a tool widely used in both veterinary and
93 human medicine. Apart from the fact that it only allows indirect detection of infection
94 through the demonstration of antibody production, it requires a detectable and stable
95 humoral response. In a context of multiple ERV copies impairing the development of
96 a XRV-specific humoral response, antibody detection in JSRV or ENTV infected
97 animals is not a reliable tool to establish the infectious status [7–10].

98 Therefore infection can only be detected *ante or post mortem* using molecular
99 approaches, *i.e.* PCR and/or RT-PCR [7,11]. The genetic diversity of JSRV and ENTV
100 is only partially known, and before our recent study reporting on 29 JSRV and 24 ENTV
101 partial and full proviral sequences [12], only a few dozen complete sequences were
102 available in the databases, i.e. nine complete sequences of JSRV isolated in Africa,
103 North America, Europe and Asia [13–17], and 50 complete or near-full length ENTV
104 genomes isolated in Canada and Europe for ENTV-1 [18,19] and in Europe and Asia
105 for ENTV-2 [20–26], including sequences not associated with accessible publications
106 or unpublished.

107 The widespread use of high-throughput sequencing tools has made pathogen
108 sequences widely available. In theory, detecting viral or proviral genomes using
109 targeted molecular approaches is straightforward, given the multiple bioinformatic
110 tools available for designing primers and probes. However, when dealing with the
111 coexistence of genetically closely related ERV family II.5 and XRVs, it is crucial to
112 ensure the strict XRV specificity of the primers or probes. To optimize the molecular
113 XRV detection tools in regards to published studies, we reviewed multiple reports,

114 focusing on the molecular detection and sequencing tools used and their relevance in
115 the context of the coexistence of XRVs with ERV II.5 *loci* [6]. A recent study of all
116 available sequences in databases allowed us to identified sequences wrongly
117 identified as exogenous JSRV or ENTV despite the absence of the YXXM motif in the
118 region of the *env* gene encoding the intracytoplasmic tail (CT), suggesting their
119 endogenous origin [12]. The YXXM motif is an essential oncogenic determinant, and
120 a genetic marker of exogenous sequences, that is strictly absent from all the ERV II.5
121 Oa and Ch sequences identified up to date [6,12,18,27]. On the other hand, some
122 studies have relied on RNAs to specifically detect XRVs [20,23,28–31]. This approach
123 assumes that ERVs are not expressed in tissues, which is risky as we will show in this
124 study.

125 In a large retrospective study based on published and unpublished sequences
126 included in the public archives, we questioned the truly exogenous nature of the
127 detected and sequenced viral genomes, after highlighting errors in the annotation of
128 sequences unduly identified as XRV. To this end, we defined the regions of the JSRV
129 and ENTV genomes specific to XRVs. We then reanalysed the available sequences
130 and published amplification tools to determine their specificity, verified the XRV
131 specificity of primers reported in the literature, and proposed a systematic approach
132 with rigorous controls to ensure the exogenous nature of the sequences. We apply our
133 methodology to case studies reporting on the detection of JSRV or ENTV in ticks and
134 mosquitos [32–37] using metagenomics or virome approaches and their potential
135 transmission by those vectors.

136 Our study raises questions about the robustness of the virus discovery in the context
137 of XRVs/ERVs coexistence in small ruminants and the overall challenge in

138 metagenomic and transcriptomic studies in the presence of ERVs and more globally
139 endogenous viral elements (EVEs) [38].

140 Results

141 The sections of the genome that differ between ERVs and 142 XRVs are limited

143 To determine the diversity of XRV sequences, we compiled a dataset comprising 79
144 complete sequences of JSRV, ENTV-1, ENTV-2 and ERV II.5 consensus sequences.
145 Analysis of the variation, in the percentage of identity of the XRV genomes against the
146 ERV II.5 Oa consensus for the JSRV and ENTV-1, which infect sheep, or the ERV II.5
147 Ch consensus for the ENTV-2, which infects goats, clearly showed that regions with
148 less than 80% identity between the XRVs and the ERVs are restricted to four
149 discriminating regions, DR1 to DR4. The other regions of the genome do not allow for
150 discrimination between XRVs and ERVs (Fig1). The confidence interval for the ENTV-
151 2 percentage identity is higher than those calculated for JSRV or ENTV-1. In the non-
152 discriminating *pro* and *pol* regions of ENTV-2, the diversity is greater than that
153 observed in the equivalent regions of JSRV and to a lower extent to ENTV-1, notably
154 due to sequences that are genetically close to the goat ERV consensus (S2 Fig, *e.g.*
155 sequences KU258870.1, MK210250.1, ON843769.1, MK164396.1). The DR2 region
156 is less marked in ENTV-1 compared to JSRV and ENTV-2, with a percentage of
157 identity higher than 80%. In addition to the nucleotide polymorphism, the DR1, 3 and
158 4 regions, displayed specific insertion/deletion (Indels) patterns that can discriminate
159 between exogenous and endogenous sequences (S3 Fig). The insertion in DR2 is
160 only present in ERV II.5 Ch and its length varies between ERV copies (S3B Fig).

161

162 **Fig 1. XRV are genetically close to ERVs.** The identity score was calculated from a
163 multiple alignment (MAFFT) of XRV sequences against a consensus sequence of ERV
164 II.5 Oa for JSRV and ENTV-1 and ERV II.5 Ch for ENTV-2. The average identity
165 percentage was calculated using a 100-base pair window and plotted in steps of 10.
166 A 95% confidence interval was represented for each virus, using a bootstrap-type
167 repetition approach. The 286 primers (grey triangles ▼), reported in publications (S2
168 Table) and used for the detection of XRV, were positioned with a tolerance of 4
169 mismatches. Primers tested in this study are identified by green triangles (▼). DR1-
170 DR4: discriminating regions 1-4.

171

172 Of the 286 PCR primers/probes listed in the 109 published studies, only 28% (79 out
173 286) were qualified as discriminating between XRVs and ERVs by our *in silico* analysis
174 (S2 Table). Notably, among the 286 primers, 74 (26%) are in the *pro* or *pol* genes,
175 which are regions that are highly similar between XRV and ERV sequences. Similarly,
176 less than one third of the primers in R / U5 region are specific. Therefore, in order to
177 minimize the risk of amplifying ERVs instead of XRV, they must be combined with XRV
178 specific primers.

179 Phylogenetic reconstructions reveal the challenge of 180 correctly classifying XRV

181 Phylogenetic trees, were reconstructed in the *pol* region (Fig 2), which weakly
182 discriminates between XRVs and ERVs, as well as in the DR1-DR2 (Fig 2B) and the
183 DR3-DR4 (Fig 2C) segments from 32 JSRV, 14 ENTV-1, 45 ENTV-2, 27 ERV II.5 Oa

184 and 10 ERV II.5 Ch sequences were extracted from GenBank and supplemented by
185 sequences identified on the assemblies of the *Ovis aries* (ARS-UI_Ramb_v2.0) and
186 *Capra hircus* (ARS1.2) reference genomes [6].

187

188 **Fig 2. DR1-DR2 et DR3-DR4 are sufficient to classify JSRV, ENTVs and ERV**
189 **sequences.** Full-length sequences XRVs and ERVs available on GenBank by July
190 2025 and ERV copies annotated in *Capra hircus* and *Ovis aries* were used for
191 phylogenetic reconstructions. The maximum likelihood trees generated using 10,000
192 ultrafast bootstraps were rooted on the Bt ERV (Bos taurus ERV) family II.4 consensus
193 sequence [6] for **A.** the *pol* gene, **B.** the 360-nt DR1 - DR2 region and **C.** the 449-nt
194 DR3 to DR4 region. The scale bar indicates the number of substitutions per site. Black
195 triangles indicate sequences that have been referred to exogenous JSRV or ENTV
196 despite the absence of the YXXM oncogenic motif in the TM region.

197

198 These analyses revealed that the segregation of viral species varies considerably
199 depending on the region considered. The *pol* region did not permit a clear distinction
200 between XRV and ERV II.5 (Fig 2A). Conversely, the DR1-DR2 and DR3-DR4 regions
201 (Fig 2B-C) enabled the different viral forms to be separated into XRVs and ERVs.
202 However, 17 of the XRV sequences were grouped with the ERV sequences,
203 regardless of whether the trees were reconstructed using the DR1-DR2 or DR3-DR4
204 regions, this calls into question their exogenous origin. Some of the potentially
205 misidentified sequences presented a clear ERV pattern, including specific
206 insertions/deletions (indels) in the DR1-DR4 segment and the lack of the YXXM motif
207 in Env (e.g. MK164396 and MK210250 for ENTV-2 or DQ838494 and MZ931278 for

208 JSRV, Fig 3). The MK210250 sequence displayed a very strong sequence identity
209 (>96%) with the ERV II.5 *Capra hircus* consensus sequence in DR4, whereas the
210 MK164396 sequence did not show a clear pattern, being equally distant from the
211 exogenous and endogenous reference sequences (with an identity percentage
212 ranging from 80 to 83%). Two JSRV sequences, DQ838494 & MZ931278, which
213 cluster with ERVs had DR4/U3 sequences that are very different from the ERV II.5
214 consensus sequence with 35% and 71% identity respectively, as well as from the
215 JSRV-FR2054 (PP707050.1) reference sequence with 33% and 52% identity,
216 respectively. The BLAT of the DR4 sequence of DQ838494 against the sheep genome
217 (Oar_v4.0/oviAri4) resulted in multiple hits. The first hits (with over 95% identity)
218 corresponded to LINE sequences of the RTE-BovB family, suggested the unmonitored
219 amplification of another transposable element.

220

221 **Fig 3. Example of wrongly annotated XRV retroviruses** Viral genome sequences
222 of JSRV (DQ838494 ; MZ931278) or ENTV (MK164396 ; MK210250) strains were
223 aligned (MAFFT) with viral genomic reference sequence of *Capra hircus* and *Ovis*
224 *aries* II.5 ERV consensus sequences [6], JSRV clade I (FR2054; PP707050.1), clade
225 II (FR989; PP707047.1), ENTV-1 (FR4403, PP669280.1) and ENTV-2 (FR3824,
226 PP669281.1) in **A.** DR1, **B.** DR2 , **C.** DR3 and **D.** DR4. Only nucleotides distinct from
227 the ERV II.5 Ch (top sequence) are indicated, identical nucleotides are marked by a
228 dot. The position on the alignment is indicated on top.

229

230 Different combinations of mixed XRV/ERV patterns can be observed, such as DR1
231 and DR3 insertions ("ERV like") for ENTV-2 ON843769 and MZ931277, and DR3

232 deletion (“XRV like”) for PP682590. A group of sequences reported as ENTV-2
233 (KU258870 to KU258880) and integrated into the caprine ERV II.5 phylum does not
234 display the described typical ERV indels profile. Although only KU258870 lacks the
235 YXXM motif, they were still more similar to ERVs in DR1-DR2 and DR3-DR4 regions.
236 No accessible articles describing the conditions under which the sequences were
237 generated were available for any of these sequences except DQ838494 [16] and
238 MK164396 [25], which cluster with ERV II.5 sequences. In the cases of DQ838494
239 and MK164396, the associated primer sets were predicted to have very low to no
240 exogenous specificity for most primer pairs (S2 Table). This was likely the original
241 cause of the misidentification of these sequences. These genomes, which are most
242 probably ERVs rather than XRV or ERVs/XRV artificial chimeras, have been used as
243 reference sequences in other studies to develop molecular tools [20,21,25].

244 These analyses highlight the importance of selecting specific regions for detecting
245 XRVs without interfering with ERVs, which are present in multiple copies in ovine and
246 caprine genomes.

247 Reliability of XRV detection in an ERV context

248 Numerous published studies have reported the detection of JSRV and/or ENTV using
249 primers located in regions that are conserved between XRV and ERVs. This makes it
250 impossible to exclude the amplification of ERVs (S2 Table). To illustrate this challenge,
251 fourteen primer sets, defined as specific to JSRV or ENTVs were selected (S3 Table).
252 Specific primers for XRVs were included as specificity control [12].
253 The primers were defined by the following 3 criteria. The first one was the ability of
254 primers to detect either exogenous ENTV-2 (pairs 1-10) or JSRV (12-15) according to
255 the authors (S2-S3 Tables). The second criterion was the specificity of the primer

256 predicted through XRV and ERV sequences alignment. The third criterion relied on
257 the ability of primers to produce an amplicon of the expected size only from genomic
258 DNA extracted from JSRV- or ENTV-2-induced tumours and not from uninfected
259 ovine, caprine and human cells.

260 The theoretical specificity of the primers was predicted by aligning them with the XRV
261 and ERV sequences published from the public databases (S1-S2 Tables). Of the ten
262 pairs selected for ENTV-2, primer alignment identified seven pairs (#1, 3, 4, 5, 6, 7, 8)
263 that were non-specific for XRV, due to high homology with ERV sequences. Only three
264 pairs (2, 9, and 10) were specific for ENTV-2. Of the four pairs selected for JSRV, only
265 pair #14 was predicted to be specific for XRV. The primer pairs were then evaluated
266 for their ability to specifically amplify XRV, with amplicon generated only from gDNA
267 extracted from ENTV-2 or JSRV-induced tumours, and conversely to fail to produce
268 signal from gDNA extracted from IDO5, TiGEF or HeLa cells. Amplicons of the
269 expected size from all the gDNAs tested, whether extracted from tumours induced by
270 ENTV-2 as well as by JSRV or from uninfected ovine, caprine were generated for the
271 seven primer pairs # 1, 3, 4, 5, 6, 7, 8 predicted to be non-specific for ENTV-2. More
272 surprisingly, DNA was amplified with the primer pair #4 for human cells. Sequencing
273 confirmed this to be HERV-K (S4 Fig).

274 Similarly, of the four primer pairs tested for JSRV (12-15), only one pair (#15) was
275 found to be strictly specific, allowing amplification only from lung tumour gDNA; no
276 signal was observed from ENTV-2-induced nasal tumours or from uninfected human,
277 goat and sheep cells, confirming the perfect discrimination between ERVs and
278 exogenous retroviruses (Fig 4). In contrast, the other three primer pairs (#12, 13, 14)
279 produced an amplicon regardless of the gDNA or infection status. This confirms that

280 the published XRV primers are non-specific, enabling , indiscriminate amplification of
281 XRV and ERV sequences.

282

283 **Fig 4. Lack of specificity of selected XRV primers.** We analysed the 'XRV
284 specificity' of fourteen published primer pairs (01 to 10 and 12 to 15) according to the
285 authors' statement ('Publication'), our *in silico* analysis ('Prediction') and their profil of
286 detection in PCR ('Experiment'). The "XRV infected" reference panel consisted of
287 genomic DNAs extracted from a nasal tumour induced by ENTV-2 (FR3824, GenBank
288 accession PP669281.1) and lung cancers induced by clade I (FR2054; GenBank
289 accession PP707050.1) or clade II (FR989; GenBank accession PP707047.1) JSRV.
290 The "XRV non-infected" reference panel consisted of genomic DNAs extracted from
291 goat (TiGEF), sheep (IDO5) and human (HeLa) cell lines. Y: Yes; N: No. NTC: No
292 Template Control.

293

294 Amplicons obtained from DNA extracted from IDO5 sheep cells were sequenced.
295 Aligning the obtained sequences with the JSRV and ENTV-2 references sequences
296 (JSRV: FR2054 - PP707050; FR989 - PP707047; ENTV-2: FR3824 - PP669281) and
297 ERV II.5 confirmed their endogenous nature as evidenced by their high homology with
298 ERV II.5 family sequences (S5 Fig).

299 To unequivocally established their XRV or ERV nature, amplicons obtained with
300 primers containing the discriminating regions DR1 in *gag* (pair #1) and DR3 in *env*
301 (pair #13), were sequenced, and aligned against XRVs and ERV II.5 sequences (Fig
302 5). The primer pair #1 encompassed DR1 and amplified a region a 1130 bp U5/gag
303 region. The absence of the 12-nt deletion, present only in exogenous JSRV and ENTV

304 sequences, confirms that these primers failed to amplify XRVs (Fig 5A). The absence
305 of the YXXM motif, which is only present in oncogenic XRVs, confirms the amplification
306 of ERV sequences using primers pair #13 (Fig 5B). Phylogenetic reconstruction based
307 on amplicons generated with primer sets #1 (Fig 5C) and #13 (Fig 5D) from DNA of
308 non-infected ovine IDO5 cells or JSRV-induced cancers showed that the sequences
309 were closely related to the ERV II.5 *Ovis aries* consensus sequence (ERV II.5 *Oa*),
310 confirming the amplification of ERVs as part of the sheep genome. Symmetrically, the
311 sequences of amplicons obtained from DNA of non-infected caprine TiGEF cells or
312 ENTV-induced nasal tumours were highly similar to ERV II.5 *Capra hircus* (ERV II.5
313 *Ch*) consensus sequence (Fig 5C-D)**.**

314

315 **Fig 5. Absence of exogenous DR1 and DR3 discriminatory regions in amplicons**
316 **obtained with primer pairs #01 (ENTV-2) and #13 (JSRV).** Amplicons obtained with
317 primer pairs #1 (ENTV-2) (**A** and **C**) and #13 (JSRV) (**B** and **D**) were sequenced and
318 aligned (MAFFT) with a reference sequence of ENTV-2 (FR3824, GenBank accession
319 PP669281.1), JSRV clade I (FR2054; GenBank accession PP707050.1) & II (FR989;
320 GenBank accession PP707047.1) and the consensus sequences of ERV II.5 Oa and
321 ERV II.5 Ch [4]. Only nucleotides distinct from the ERV II.5 *Ch* consensus sequence
322 (on top) have been indicated, identical nucleotides are marked by a dot. Maximum
323 likelihood (ML) trees were reconstructed using PhyML from **C.** 826-nt of the U5/gag or
324 **D.** 864-nt of the *env* amplicons with ENTV1-FR4403 sequence (GenBank accession
325 PP707036) as an outgroup for rooting. Bootstrap values (1000 replicates) are
326 expressed as a percentage and indicated at the node level. The scale bar indicates
327 the number of substitutions per site.

328

329 **Multiple tissues express endogenous sheep and goat**

330 **retroviruses**

331 Several studies have been based on amplifying JSRV and ENTV from RNAs under
332 the assumption that only exogenous retroviruses are expressed. As RNA is an
333 appropriate target for retroviruses detection, the absence of ERV expression must be
334 confirmed to rule out dual expression of XRVs and ERVs at the same sites. We
335 analysed the expression of ERV II.5 using transcriptomic data from 60 tissues of the
336 Benz2616 ewe, the source of ARS-UI_Ramb_v2.0 reference ovine genome. Short
337 sequences or k-mers were defined in DR1 in *gag* and DR3 in *env* (Fig 6, Table 3 and
338 S1 Fig) from annotated ERV II.5 copies of the ARS-UI_Ramb_v2.0 genome [6]. JSRV
339 k-mers located in DR3 and DR4 were used to detect JSRV expression from RNA-Seq
340 data from JSRV-experimentally lambs and confirm the JSRV-negative status of the
341 Benz2616 ewe (Fig 6A, Table 3 and S1 Fig) [12,47]. For each of the RNA-Seq
342 datasets, sequences with specific ERV or JSRV k-mers were counted using the BBduk
343 tool. Conversely, ERV k-mers identified small quantities of ERV transcripts in most of
344 the tested tissues, with notably higher expression in the lung and kidney (particularly
345 the internal medullary part) and oviduct (Fig 6B). Sequences identified by the ERV k-
346 mers were mapped to the consensus sequence of ERV II.5 Oa, confirming their
347 endogenous origin proven the specificity of this approach to identify transcripts (Fig
348 6C). This demonstration in sheep shows that amplifying RNAs does not guarantee the
349 sole detection of JSRV or ENTV. If the primers are not highly XRV-specific, ERVs will
350 be amplified. Additionally, the absence of cellular DNA, even as traces, must be

351 carefully controlled to prevent the amplification of ERV copies, present in multiple
352 copies.

353

354 **Fig 6. Expression of ERV family II.5 in tissues. A**. K-mers localization on the JSRV
355 provirus. kERV-DR1 and kERV-D3 are specific to ERV II.5 Oa and located in the DR1
356 (*gag*) and DR3 (*env*) discriminating regions, respectively. kJSRV-DR3 and JSRV-DR4
357 are specific to JSRV and located in DR3 (*env*) and DR4 (U3). **B**. The number of reads
358 containing one of the four selected k-mers was calculated for each tissue or organ.
359 The samples were grouped by physiological system and visualised using a colour
360 code. JSRV-infected and uninfected control sample [47] were added and labelled as
361 "Lung_JSRV_infected" for lung RNA-Seq data of JSRV-JS21-infected lamb or
362 "Lung_JSRV_uninfected" for uninfected control lambs. **C.** Reads containing kERV-
363 DR1 and kERV-DR3 k-mers were mapped on the ERV II.5 Oa consensus sequence
364 and visualised on IGV.

365

366 The presence of JSRV and ENTV in arthropods cannot be
367 not confirmed

368 Six recent studies identified small ruminant XRV sequences [32–37] in insect vectors
369 using global approaches, such as metagenomics, transcriptomics and whole RNA-
370 Seq enriched for viral RNA. We used these datasets to challenge both our strategy for
371 specifically detecting XRVs in a context of coexistence of both XRV and ERVs in the
372 same individuals and the hypothesis of a potential vectorisation. Those approaches
373 rely on the BLASTn of the *de novo* assembled genomes to identify reference

374 sequences. Two studies made the reference matches available [33,36]. While
375 analysing the different datasets, we observed that identification of sequences
376 deposited in GenBank can be misleading. For example, MN564750.1 used as a
377 reference, is associated in GenBank with the organism "Enzootic nasal tumor virus 2"
378 (Taxonomy ID: 2913605), ID which also includes "Endogenous enzootic nasal tumor
379 virus". MN564750.1 is identified as "Enzootic nasal tumor virus 2 isolate enENTV-FJ2
380 genomic sequence". A scientist familiar with these viruses would recognise that the
381 name of the isolate 'enENTV-FJ12' corresponds to an endogenous (en) virus.
382 However, this is confusing, particularly in the absence of an associated article or any
383 further information about the origin in the deposit entry. We clearly identified ERV
384 sequences wrongly tagged as XRV in public databases such as MK210250 (Figs 2
385 and 3) or KT266728 (S6 Fig) used as a reference respectively for the detection of
386 ENTV-2 [33] and JSRV [36] which both lack the sequence coding for the YXXM motif.
387 Overall, this detailed initial analysis highlights the importance of carefully selecting the
388 reference sequence to exclude ERV sequences.

389 In their study [36], the authors identify both sequences of JSRV and ENTV-2 within
390 mosquitoes but only validated the presence of JSRV. While the amplification and
391 sequencing led to the identification of the sequence as "enJSRV", the validation was
392 initially biased as primers (S2-S3 Tables) not specific for exogenous viruses were
393 designed based on the sequence initially matching with their reference. The non
394 specificity of primers #16 and #17 was confirmed using the same experimental design
395 with reference samples of DNA extracted from XRV-induced tumours, negative sheep
396 and goat controls, including DNA extracted from different mosquito species. The
397 amplification pattern was non-specific, with amplification in both uninfected and

398 infected samples (Fig 7A). The #16 and #17 primer sets amplified regions confirmed
399 to be of ERV origin by sequencing. The DR3 amplicon obtained with PCR #16 (Fig
400 7B) does not contain the insertion specific of XRVs nor the sequence coding for the
401 YXXM motif; the DR4 amplicon obtained with PCR #17 (Fig 7 A-C) has both the size
402 and sequence compatible with the ERV II.5 consensus. Neither the sequence nor the
403 accession number were made available for the “nearly complete sequence” of ENTV-
404 2 identified in mosquitoes. However the authors reported that the sequence was
405 closely related to the GDQY2017 Chinese strain (accession number MK164396), a
406 sequence that we identified as ERVs, questioning the XRV nature of the ENTV-2
407 sequence identified in this study (Figs 2 and 3) [36].

408

409 **Fig 7. Molecular detection of JSRV and ENTVs in mosquitoes**. **A.** Evaluation of
410 the specificity of primer pairs # 16 and #17 on genomic DNA extracted from JSRV or
411 ENTV tumours, from uninfected *sheep (IDO5) and goat (TIGEF)* cell lines, and from
412 *Aedes aegypti (Ae)* and *Culex Quique/asciatus (Cq/a*). The amplicons obtained with
413 primer pairs #16 (**B**) and #17 (**C**) were sequenced and aligned against ERV II.5, ENTV
414 and JSRV reference sequences. Only nucleotides distinct from the ERV II.5 *Ch*
415 consensus sequence (on top) have been indicated, identical nucleotides are marked
416 by a dot.

417

418 In a recent study [35], ENTV was amplified and sequenced from ticks collected in
419 Pakistan. A nearly full-length proviral genome (OR991120) was amplified (Fig 8A).
420 The sequence displayed 98% and 92 % overall nucleotide identity respectively with
421 the caprine and sheep ERV II.5 consensus, but less than 89% with JSRVs and ENTVs.

422 The DR3 and DR4 regions were unavailable. However, the DR1 and DR2 regions
423 displayed indels characteristics of ERVs (Fig 8C-D), as well as an ERV-specific partial
424 insertion in DR2 region. These findings suggest that the “provirus” was amplified from
425 a goat ERVs. The single set of primer targeting the *gag/ pol* was not predicted as
426 specific of XRVs, allowing an amplicon from both XRV infected and uninfected sources
427 (Fig 8B). The DR1 and DR2 sequencing of the amplicon confirmed the ERV nature of
428 the sequence (Fig 8C-D).

429

430 **Fig 8. Molecular detection of ENTV in ticks. A**. The partial OR991120 proviral
431 sequence, missing the LTRs and the DR3 region, reported in ticks [35] was aligned
432 with II.5 ERV Oa and Ch consensus sequences [6], JSRV clade I (FR2054; GenBank
433 accession PP707050.1), clade II (FR989; GenBank accession PP707047.1), ENTV-
434 1(FR4403, GenBank accession PP669280.1) and ENTV-2 (FR3824, GenBank
435 accession PP669281.1). The black and grey bars correspond respectively to the
436 differential or identical nucleotides. **B**. Evaluation of the primer specificity. The
437 amplicon #11 was sequenced and aligned against proviral sequences of JSRV, ENTV
438 and ERV II.5. **C.** Alignment of the DR1 region. **D.** Alignment of the DR2 region.

439

440 Three studies identified ENTV-2 in ticks isolated from cattle [32], JSRV from sheep
441 [37], ENTV-2 and JSRV from ticks isolated from yaks and ENTV-1 from Tibetan sheep
442 [34]. Unfortunately, neither data on the overall or DR regions coverage were available,
443 nor molecular validation of the presence of JSRV and ENTVs with XRV specific tools
444 were reported, only information regarding the abundance of the reads were available
445 for [32] and [34]. Therefore, the conclusions that can be drawn about the exogenous

446 nature of these sequences are limited, without further investigations. *A contrario* a
447 thorough checking based on the current recommendation can dispel doubts about the
448 nature of the strains detected by these high-throughput approaches. We therefore
449 collaborated with the authors to rework the preprint [33], which initially described
450 ENTV-2 within ticks. One of the tick metagenome samples displayed coverage of the
451 ENTV-2 provirus of over 80%, thus enabling to distinguish between ERV/XRV and
452 clearly identifying the DR1-3 regions associated with ERV. DR4 coverage was lower
453 but also suggested the detection of ERV. Phylogenetic analysis confirmed these
454 conclusions, as the consensus sequence clustered with the ERV sequences (S7 Fig).

455 # Discussion

456 Accurate detection of β-retroviruses responsible for respiratory cancers in sheep and
457 goats is a critical prerequisite for controlling these diseases in livestock. This task is
458 complicated by the coexistence of exogenous retroviruses (JSRV and ENTV) with
459 numerous copies of endogenous retroviruses belonging to the ERV II.5 family in the
460 genome of sheep and goats. Molecular diagnostic approaches must therefore allow
461 unequivocal detection of XRV and therefore target regions that clearly discriminate
462 between ERVs and XRVs. Insufficient consideration of this constraint has directly
463 impacted on the specificity of molecular assays, the interpretation of phylogenetic
464 relationships, and the integrity of sequence annotations.

465 Early studies, based on a limited number of available sequences, suggested that
466 regions 1 to 4 could discriminate between ERVs and XRVs due to their low sequence
467 homology [5,19]. Building on these observations, we conducted an extensive analysis
468 integrating available XRV and ERV sequences with *in silico* annotation of ERV II.5 loci

469 in sheep and goat assemblies, that allowed us to define four discriminating segments
470 (DR1-DR4) that robustly discriminate exogenous from endogenous retroviruses. DR1
471 and DR2 localize in the 5‘gag region, DR3 in the 3’ terminus of *env*, and DR4 to U3.
472 Thus, they are prime targets for virus detection, reconstruction of phylogenetic
473 relationships and sequencing of near-full length of exogenous β-retroviruses. As we
474 established in this study from *in silico* analysis of primers reported in the literature,
475 targeting other regions with limited variation between ERVs and XRV forms poses a
476 risk of ERV detection.

477 As frequently reported in the literature, primers targeting conserved regions shared
478 between ERVs and XRVs are inherently non-specific and prone to amplifying
479 endogenous sequences. As we established in this study, most primers used to detect
480 JSRV or ENTV are unable to distinguish between exogenous and endogenous
481 sequences present in animal genomes and if used must be paired with XRV specific
482 primers. In a similar way, the growing use of high-throughput sequencing without
483 adequate discrimination criteria has amplified this problem. In recent years, this
484 methodological flaw has led to widespread mis-annotation of ERVs as infectious JSRV
485 or ENTV, distorting evolutionary analyses and misleading the development of
486 molecular tools.

487 Misinterpretation extends beyond host samples. Recent reports suggesting JSRV or
488 ENTV presence in ticks or mosquitoes may most likely reflect the detection of goat or
489 sheep DNA acquired from blood meal rather than true viral infection. As we have
490 shown there is no evidence that arthropods could serve as reservoirs or vectors for
491 JSRV and ENTV. Xenosurveillance may help to identify infection [36] but the clear
492 frontier with ERVs has to be drawn.

493 The distinction between XRV and ERV is often blurred in sequence databases, such
494 as GenBank, due to the presence of redundant and inconsistent taxonomic identifiers
495 that merge XRV and ERV. While a single taxonomic ID (69576) is defined for ENTV-
496 1, JSRV is classified within the taxonomic ID 47898 (recognised by the ICTV), which
497 also includes the "Endogenous Jaagsiekte retrovirus" (also classified with the *Ovis*
498 *aries*, taxonomic ID: 9940). A subclass "Exogenous Jaagsiekte sheep retrovirus"
499 (Taxonomic ID: 47898) is also reported, but this only contains 6 sequences. For ENTV-
500 2 the problem is even more complex. Recently, four taxonomic IDs coexisted for the
501 same virological entity, but taxonomic ID 2762664 (Endogenous enzootic nasal tumor)
502 and taxonomic ID 239365 (Enzootic nasal tumour virus of goats) were recently merged
503 with taxonomic ID 2913605 (Enzootic nasal tumor virus 2). The fusion of taxonomic ID
504 2762664 with 2913605 artificially grouped XRV and ERV sequences, whereas the
505 latter could be defined as part of the goat genome with identifier 9925 (*Capra hircus*).
506 Finally, the only singularity of taxonomic ID 2584748 is that it is defined by its common
507 name in US English, with "tumour" instead of "tumor".

508 The classification of ERVs based on whether they are considered part of the virus or
509 the host is still a challenge, not limited to retroviruses in small ruminants. As an
510 example, porcine endogenous retroviruses are associated in GenBank either to their
511 host genome, *Sus scrofa* (Taxonomic ID 61673) or to the viral entity PERV (Porcine
512 endogenous retrovirus) (Taxonomic ID: 61673) subdivided in 11 subclasses with their
513 own taxonomic IDs. Brait and colleagues [38] suggest a rational solution to bypass
514 this challenge by adding a second taxonomic identifier. In this context, referring to ERV
515 II.5 with the taxonomy ID of the host in which they have been identified and a second
516 taxomic ID related to the closest XRV offers a pragmatic solution.

517 Finally, genome assembly approaches using short amplicon sequencing are ill-suited
518 to contexts where ERVs and XRVs coexist, as they cannot exclude chimeric
519 reconstructions. Long read sequencing technologies are therefore preferable an less
520 prone to generate *in silico* artefacts [12]. Regardless the approach used, the genetic
521 nature of the DR1 to DR4 discriminating regions is a minimal requirement for
522 classifying sequences as exogenous. Hallmarks features such as deletions in DR1/
523 DR2 regions as compared to ERV II.5, and the presence of the exogenous oncogenic
524 YXXM motif in DR3 (strictly absent in ERV) provide unambiguous evidence of
525 exogenous origin.

526 Although most of the complete sequences of JSRV and ENTV present in GenBank
527 possess these motifs indicating a probable exogenous origin, doubts remain about the
528 non-discriminatory regions such as the end of *gag*, *pro*, *pol* and the beginning of *env*.
529 For example, a recent study suggests possible recombination between different
530 strains of ENTV-2, precisely in the *pro* and *pol* regions, in which the absence of the
531 XRV/ ERV discriminatory region complicates amplification and the specific
532 identification of sequences of exogenous origin [21]. In this case, the reconstruction of
533 chimeric XRV/ ERV sequences cannot be ruled out.

534 The DR1-DR4 regions exhibit sufficient polymorphism to resolve viral clades and
535 geographic lineages. Updated diagnostic tools must therefore balance specificity for
536 exogenous viruses with coverage of known diversity.

537 In conclusion, we urge the stringent validation of the molecular tools used to detect
538 JSRV, ENTV-1, and ENTV-2. Primer pairs should include at least one primer located
539 in discriminating regions DR1–DR4, and the absence of amplification from DNA of
540 uninfected ovine and caprine cells specificity must be confirmed to establish

541 specificity. RNA-based detection alone is insufficient to exclude ERV contamination,
542 particularly in complex clinical samples and if we consider that ERV expression is
543 present in various tissues. Finally, assembled viral genomes lacking exogenous
544 hallmarks in DR1–DR4 using separated amplicons should be considered as potential
545 chimeric genomes, and not the reflect of the circulating strains. Only a rigorous,
546 discrimination-based framework will restore confidence in published sequences,
547 improve database reliability, and prevent further propagation of ERV/XRV confusion.

548 Materials and Methods

549 Determination of discriminating regions between XRVs et 550 ERVs

551 Complete nucleic sequences from 30 JSRV, 14 ENTV-1 and 35 ENTV-2 sequences
552 available in GenBank (S1 Table, sequences identified with an asterisk *) were aligned
553 with the ERV II.5 consensus for *Ovis aries* for JSRV and ENTV-1, and for *Capra hircus*
554 for ENTV-2 [6]. Nucleotide alignments were performed with the 'MAFFT v7.490'
555 software [39] and processed with the 'R v4.4.1' suite to picture the variability of the
556 identity scores obtained from the comparison between XRV sequences and the ERV
557 consensus and to calculate the percentage of identity for each position in the
558 alignment, averaged over a 100 bp window with a 10 bp step. The analysis was
559 performed individually for each sequence of the alignment, and the mean percentage
560 of identity was plotted. A 95% confidence interval was estimated using a bootstrap
561 approach with the 'boot v1.3-31' suite [40], debiased and corrected for asymmetric
562 data. The limited number of samples used and the potential lack of independence
563 between sequences originated the same origins (herd, geographical location, etc.) are

564 potential biases that we have identified. Four discriminant regions (referred further as
565 DR1, DR2, DR3, DR4), were identified with a percentage of identity lower than 80%.
566 DR2 sequence variability was evaluated by aligning (MAFFT Alignment v7.490 [39])
567 copies containing the *gag* region, *i.e.* 28 ERV II.5 copies annotated from the *Ovis aries*
568 assemby (ARS-UI_Ramb_v2.0 -GCA_016772045.1) and 155 ERV II.5 copies from the
569 *Capra hircus* assembly (ARS1.2 -GCA_001704415.2), and 27 ovine and 10 caprine
570 ERV sequences recovered from GenBank [6] (S1 Table). The percentage of each
571 nucleotide among all copies was calculated at each position.

572 *in silico* and experimental evaluation of XRV primers 573 specificity

574 The localization prediction of 286 published PCR primers and probes (S2 Table)
575 reported for the detection of JSRV et ENTVs, was determined by mapping them onto
576 the respective alignments for each virus. Publications not written in English were
577 automatically translated with DeepL. A maximum of 4 mismatches from the XRV
578 sequences was allowed, and the position of each primer was extracted from the
579 alignment retaining the multi-mapped positions. Primers including additional
580 sequences, *e.g.* restriction sites, were not included. Primers only mapping on XRV
581 were defined as XRV specific whereas primers mapping on a least one copy of ERV,
582 were defined as non-specific to exogenous sequences. A selection of seventeen
583 primer pairs has been tested on various DNA templates, covering different parts of the
584 viral genomes. Fourteen of them were tested by PCR on mammalian DNAs; they
585 targeted ENTV-2 for primer pairs # 01-10 or JSRV for primers pairs 12-15 (S3 Table).
586 Their ability to detect only XRV was tested using genomic DNAs from JSRV-induced
587 lung tumours of clades I (FR2054) and II (FR989), and ENTV-2-induced nasal tumours

588 (FR3824) [12] (Table 1). To evaluate their potential for cross hybridization with ERV
589 sequences, PCRs were performed using DNAs from ovine IDO5 cells (Institut Mérieux,
590 Lyon, France), caprine TiGEF cells [41] and human HeLa cells [42] (Table 1). Primer
591 pairs 10 (ENTV-2 U3/gag) and 15 (JSRV U3/gag) have been recently published by
592 our team and shown to be highly specific for JSRV and ENTV-2, with no cross
593 hybridization with ERV sequences [12]. The amplicons obtained with pairs 01 and 13
594 for each condition (JSRV, ENTV and cell references), with pairs 03 to 08 and 14 for
595 the IDO5 cell reference and with pair 04 for HeLa cells were subjected to Sanger
596 sequencing (TubeSeq Supreme Eurofins) and aligned against XRV and ERV
597 reference proviral sequences. A BLAT search [43] on the human genome (hg38) was
598 performed to identify the nature of the amplicon sequence obtained with pair 04 from
599 human HeLa cells.

600 A similar approach was taken for the primer pairs published to target ENTV (primer
601 pair #11) and JSRV (primer pair 16 and 17) in arthropods [35,36] by adding DNA
602 extracted from an ENTV-1-induced nasal tumour (FR4403) [12] and mosquitos (*Aedes*
603 *aegypti and Culex Quique/asciatus*) that have fed on human blood. All the amplicons
604 were subjected to Sanger sequencing (TubeSeq Supreme Eurofins).

605 **Table 1. Biological samples: origin and sequences.**

Name	Biological description	Species origin	Genbank accession #	Reference
FR4403	French ENTV-1	*Ovis aries*	PP669280	(Riocreux-Verney et al., 2024)
FR3824	French ENTV-2	*Capra hircus*	PP669281	(Riocreux-Verney et al., 2024)
FR2054	French JSRV Clade I	*Ovis aries*	PP707050	(Riocreux-Verney et al., 2024)
FR989	French JSRV Clade II	*Ovis aries*	PP707047	(Riocreux-Verney et al., 2024)
IDO5	Ovine dermal fibroblasts	*Ovis aries*	NA	NA
TiGEF	T-immortalized Goat Embryonic Fibroblasts	*Capra hircus*	NA	(Da Silva Teixeira et al., 1997)
HeLa	Immortalized human cell line	*Homo Sapiens*	NA	(Scherer et al., 1953)
Aa	Mosquito	*Aedes aegypti*	NA	NA
Cq/a	Mosquito	*Culex quinque/asciatus*	NA	NA

ERV II.5 expression in sheep tissues

Data of mRNA-seq from 60 tissues (Table 2, Ovine FAANG project [44,45]) of the Benz2616 ewe, used to assemble the ARS-UI_Ramb_v2.0 ovine genome (GCA_016772045. 1, [46]), and of lung RNA-seq of $JSRV_{JS21}$-experimentally infected lambs and the associated uninfected controls [47] were collected from the ENA (European Nucleotide Archive) database. ERV II.5 family - specific k-mers of 21 base pairs were defined in the DR1 and DR3 regions in order to cover the largest number of copies of ERVs annotated in the ARS-UI_Ramb_v2.0 genome (Table 3 and S1 Fig) [6]. These k-mers were used to identify and count the reads corresponding to ERV sequences in the selected RNAseq data using the BBduk analysis tool (Bbtools v38.95, https://quay.io/repository/biocontainers/bbmap) by allowing two mismatches. As a control, k-mers specific to JSRV were defined in DR3 and DR4 and searched in the same RNAseq data (Table 3 and S1 Fig), as previously described [12]. The reads containing the kmers were extracted from the raw data (FastQC file), low-quality sequences and adapters were removed with Trimmomatic [48]. The sequences were then mapped (Bwa-mem, [49]) on the *Ovis aries* family II.5 consensus sequence [6]. The alignment was visualised with IGV (Integrative Genomics Viewer, [50]).

624 **Table 2. Tissues used for the ERV expression from RNA-seq data of the sheep**

625 **Benz2616. Tissues were grouped by physiological systems.**

System	Tissue	ENA accession #
Cardiac	Right ventricle	ERR3728426
	Atrioventricular valve	ERR3728429
	Right atrium	ERR3665709
	Left ventricle	SRR7612070
	Vena cava	ERR3728430
Immunitary	Spleen	ERR3728431
	Mesenteric lymph node	ERR3665711
	Prescapular lymph node	ERR3665712
	Mandibular lymph node	SRR7543059
	Alveolar macrophage	SRR6651987
Gastro-intestinal	Ileum	ERR3728427
	Ileum Peyer Patches	ERR3665710
	Cecum	ERR3665706
	Jejunum	SRR7543057
	Duodenum	ERR3650374
	Rectum	ERR3728432
	Rectum	ERR3665713
	Descending colon	SRR7543055
	Spiral colon	ERR3665714
	Esophagus	ERR3665707
	Abomasum	ERR3665705
	Abomasum pylorus	ERR3650373
	Reticulum	ERR3650375
	Rumen atrium	ERR3650376
	Rumen ventral	ERR3650377
	Omasum	SRR7543060
	Gall bladder	SRR7543056
	Liver	SRR7612072
Skin	Skin hairless	ERR3665715
	Skin of back	SRR7543062

System	Tissues	ENA accession #
Neurological	Retina	ERR3728428
	Spinal cord	ERR3728434
	Pons	ERR3728433
	Thalamus	ERR3728435
	Hippocampus	ERR3665708
	Pituitary gland	ERR3650379
	Cerebellum	SRR6651979
	Frontal cortex	SRR7612068
Renal	Adrenal medulla	SRR7543054
	Adrenal cortex	SRR6651976
	Renal medulla	SRR7543058
	Renal cortex	SRR7612071
Respiratory and buccal	Tongue	SRR7612076
	Soft palate	ERR3650378
	Epiglottis	SRR6651978
	Palatine tonsil	SRR7612075
	Lung	SRR6651986
Urinary	Urinary bladder	ERR3728424
	Urethra	ERR3665716
	Ureter	SRR7543063
Endocrine	Mammary gland	ERR3728425
Genital	Uterus	ERR3665717
	Oviduct	SRR7543061
	Ovary	SRR6651991
	Vagina	SRR7612077
Muscular	Biceps femoris	SRR6651988
	Semimembranosus	SRR6651990
	Longissimus dorsi	SRR7612073
	Supraspinatus	SRR7612074
	Diaphragm	SRR7612069

626

627 **Table 3. k-mer sequences and localization for the identification of tissue**

628 **expression of ERVs of family II.5 or the exogenous virus.**

Target	Discriminating region (DR)	Name	5' - 3 ' sequence
ERV	DR1	kERV-DR1	TATGCTGTTCCCGAGGGGGTT
	DR3	kERV-DR3	GAGAGTTTTAATACATAAAAA
JSRV	DR3	kJSRV-DR3	GAGAGTTGAAATGCTACATAT
	DR4	kJSRV-DR4	TCTGATTATGTAAGAATCCGG

629

630 # Alignment and phylogenetic analyses

631 The alignments of *pol*, DR1-DR2, DR3-DR4, complete genomes and sequenced
632 amplicons were carried out using MAFFT Alignment v7.490 [39] and Geneious Prime
633 software (v 2025.0.2). Maximum Likelihood (ML) phylogenetic trees in the *pol*, DR1-
634 DR2, DR3-DR4 regions were generated using IQ-TREE v1.5.3 [51] with 10,000
635 ultrafast bootstrap and rooting on the BT ERV (Bos taurus ERV) family II.4 consensus
636 sequence [6]. ML-type phylogenetic trees (PhyML 3.3.20180621, Jukes Cantor
637 substitution model) of the *gag* (pair #01, 826nt) and *env* (pair #13, 864 nt) sequences
638 were created using the ENTV1-FR4403 sequence (GenBank #PP669280, [12]) for
639 rooting, with 1000 iterations (bootstraps) and edited through the iTOL software.

640 Publicly available sequences used in the study are reported in S1 Table. ERV copies
641 from the family II.5, annotated in the *Capra hircus* assembly ARS1.2
642 (GCA_001704415.2) and the *Ovis aries* assembly ARS-UI_Ramb_v2.0
643 (GCA_016772045.1), were retrieved from [6]. The partial proviral sequence
644 OR991120 described in [35] and the partial *env* sequence KT266728 [36] were also
645 analyzed.

646 # Acknowledgements

647 We thank Loïc Schwaller and Emmanuelle Lerat for the scientific advice; Vincent
648 Raquin and Barbara Viginier for providing us the mosquitoes. This work was
649 performed using the computing facilities of the CC LBBE/PRABI.

650 # Funding

651 This research was funded by ANR, grant ANR-22-CE35-0002-01 and by INRAE “AAP-
652 Action incitative sur priorités SSD 2021-2025”. BRV was the recipient of a VetAgro

Sup PhD grant. MV PhD fellowship was funded by ANR, grant ANR-22-CE35-0002-01.

Conflict of Interest

The authors declare that the research was conducted in the absence of any commercial or financial relationships that could be construed as a potential conflict of interest.

Author Contributions

BRV and CD realized the experiments. BRV, MV, JT, CL performed the analyses. BRV, VN, MV, CL, and JT designed the analysis. BRV, JT and CL wrote the manuscript. CL and JT conceived the project and secured the fundings. CL, JT, and VN supervised the work.

All participants contributed to the design and implementation of the research, participated to the interpretation of the data, and revised the manuscript.

Bibliography

1. Sigurdsson B. Adenomatosis of sheep's lungs; experimental transmission. Arch Gesamte Virusforsch. 1958;8: 51–58. doi:10.1007/BF01242312

2. De Las Heras M, Ortín A, Cousens C, Minguijón E, Sharp JM. Enzootic Nasal Adenocarcinoma of Sheep and Goats. In: Fan H, editor. Jaagsiekte Sheep Retrovirus and Lung Cancer. Berlin, Heidelberg: Springer Berlin Heidelberg; 2003. pp. 201–223. doi:10.1007/978-3-642-55638-8_8

3. Griffiths DJ, Martineau HM, Cousens C. Pathology and Pathogenesis of Ovine Pulmonary Adenocarcinoma. Journal of Comparative Pathology. 2010;142: 260–283. doi:10.1016/j.jcpa.2009.12.013

4. 江锦秀，张靖鹏，林裕胜，毛坤明，游伟，黄丽丽，et al. 山羊内源性鼻内肿瘤病毒enENTV-FJ1 株分享到：全基因组测序及生物信息学分析. Chinese Journal of Preventive Veterinary Medicine/Zhongguo Yufang Shouyi Xuebao. 2020;42.

5. Palmarini M, Hallwirth C, York D, Murgia C, De Oliveira T, Spencer T, et al. Molecular Cloning and Functional Analysis of Three Type D Endogenous Retroviruses of Sheep Reveal a Different Cell Tropism from That of the Highly Related Exogenous Jaagsiekte Sheep Retrovirus. J Virol. 2000;74: 8065–8076. doi:10.1128/JVI.74.17.8065-8076.2000

6. Verneret M, Leroux C, Faraut T, Navratil V, Lerat E, Turpin J. A genome-wide study of ruminants uncovers two endogenous retrovirus families recently active in goats. Mobile DNA. 2025;16: 4. doi:https://doi.org/10.1186/s13100-024-00337-6

7. Ortín A, Minguijón E, Dewar P, García M, Ferrer LM, Palmarini M, et al. Lack of a specific immune response against a recombinant capsid protein of Jaagsiekte sheep retrovirus in sheep and goats naturally affected by enzootic nasal tumour or sheep pulmonary adenomatosis. Veterinary Immunology and Immunopathology. 1998;61: 229–237. doi:10.1016/S0165-2427(97)00149-9

8. Hudachek SF, Kraft SL, Thamm DH, Bielefeldt-Ohmann H, DeMartini JC, Miller AD, et al. Lung Tumor Development and Spontaneous Regression in Lambs Coinfected With Jaagsiekte Sheep Retrovirus and Ovine Lentivirus. Vet Pathol. 2010;47: 148–162. doi:10.1177/0300985809352787

9. Caporale M, Martineau H, De las Heras M, Murgia C, Huang R, Centorame P, et al. Host Species Barriers to Jaagsiekte Sheep Retrovirus Replication and Carcinogenesis. J Virol. 2013;87: 10752–10762. doi:10.1128/JVI.01472-13

10. Walsh SR, Stinson KJ, Wootton SK. Seroconversion of sheep experimentally infected with enzootic nasal tumor virus. BMC Res Notes. 2016;9: 15. doi:10.1186/s13104-015-1824-2

11. Summers C, Neill W, Dewar P, Gonzalez L, van der Molen R, Norval M, et al. Systemic immune responses following infection with Jaagsiekte sheep retrovirus and in the terminal stages of ovine pulmonary adenocarcinoma. J Gen Virol. 2002;83: 1753–1757. doi:10.1099/0022-1317-83-7-1753

12. Riocreux-Verney B, Verneret M, Diesler R, Dolmazon C, Gineys B, Cadoré J-L, et al. Association between genetic clades and cancer prevalence suggested by French-wide study of oncogenic small ruminant β-retrovirus diversity. Front Cell Infect Microbiol. 2024;14. doi:10.3389/fcimb.2024.1466333

13. York DF, Vigne R, Verwoerd DW, Querat G. Nucleotide sequence of the jaagsiekte retrovirus, an exogenous and endogenous type D and B retrovirus of sheep and goats. J Virol. 1992;66: 4930–4939. doi:10.1128/jvi.66.8.4930-4939.1992

716 14. Palmarini M, Sharp JM, de las Heras M, Fan H. Jaagsiekte Sheep Retrovirus Is
717 Necessary and Sufficient To Induce a Contagious Lung Cancer in Sheep. J Virol.
718 1999;73: 6964–6972.

719 15. DeMartini JC, Bishop JV, Allen TE, Jassim FA, Sharp JM, de las Heras M, et al.
720 Jaagsiekte Sheep Retrovirus Proviral Clone JSRVJS7, Derived from the JS7
721 Lung Tumor Cell Line, Induces Ovine Pulmonary Carcinoma and Is Integrated
722 into the Surfactant Protein A Gene. J Virol. 2001;75: 4239–4246.
723 doi:10.1128/JVI.75.9.4239-4246.2001

724 16. Shuying L, Xueen M, Jingwei Q, Yu W. Cloning and sequencing analysis of the
725 complete genome of jaagsiekte sheep retrovirus inner mongolia strain. Zhongguo
726 Bing du xue= Virologica Sinica. 2006;21: 443–448.

727 17. Yadav EJ, Prabhakar YK, Shanmugam G, Vijayakumar P, Kumar MVJ,
728 Vijayakumar N, et al. Whole genome characterization of Jaagsiekte Sheep
729 Retrovirus isolated from OPA infected sheep (India) and structural assessment
730 (In-silico) of proteins of JSRV. The Microbe. 2024;3: 100068.
731 doi:10.1016/j.microb.2024.100068

732 18. Cousens C, Minguijon E, Dalziel RG, Ortin A, Garcia M, Park J, et al. Complete
733 Sequence of Enzootic Nasal Tumor Virus, a Retrovirus Associated with
734 Transmissible Intranasal Tumors of Sheep. Journal of Virology. 1999;73: 3986
735 LP – 3993. doi:10.1128/JVI.73.5.3986-3993.1999

736 19. Walsh SR, Linnerth-Petrik NM, Laporte AN, Menzies PI, Foster RA, Wootton SK.
737 Full-length genome sequence analysis of enzootic nasal tumor virus reveals an
738 unusually high degree of genetic stability. Virus research. 2010;151: 74–87.
739 doi:10.1016/j.virusres.2010.04.002

740 20. Ye C, Huang Q, Chen T, Jiang J, Hou F, Xu D, et al. First detection and genotypic
741 analysis of goat enzootic nasal tumor virus 2 in Chongqing, China. Arch Virol.
742 2019;164: 1647–1650. doi:10.1007/s00705-019-04211-2

743 21. Li Y, Niu J, Liu Y, Dai Y, Ni H, Wang J, et al. Genomic Sequencing and Analysis
744 of Enzootic Nasal Tumor Virus Type 2 Provides Evidence for Recombination
745 within the Prevalent Chinese Strains. Veterinary Sciences. 2024;11: 248.
746 doi:10.3390/vetsci11060248

747 22. Li P, Cao X, Wu J, Liu X, Mao S, Yuan L, et al. Detection and analysis of enzootic
748 nasal tumor virus 2 in China. J Vet Diagn Invest. 2025;37: 244–251.
749 doi:10.1177/10406387241310204

750 23. He Y, Zhang Q, Wang J, Zhou M, Fu M, Xu X. Full-length genome sequence
751 analysis of enzootic nasal tumor virus isolated from goats in China. Virol J.
752 2017;14: 141. doi:10.1186/s12985-017-0795-4

753 24. Ortín A, Cousens C, Minguijón E, Pascual Z, Villarreal MP de, Sharp JM, et al.
754 Characterization of enzootic nasal tumour virus of goats: complete sequence and

755 tissue distribution. The Journal of general virology. 2003;84: 2245–2252.
756 doi:10.1099/vir.0.19125-0

757 25. Zhai S-L, Lv D-H, Xu Z-H, Yu J-S, Wen X-H, Zhang H, et al. A Novel Enzootic
758 Nasal Tumor Virus Circulating in Goats from Southern China. Viruses. 2019;11:
759 956. doi:10.3390/v11100956

760 26. Li P, Yin H, Cao X, Lan X, Wu J, He J, et al. Development and Application of a
761 TaqMan-Based qPCR Assay for Detecting ENTV-2 in Goats. Genes (Basel).
762 2025;16: 529. doi:10.3390/genes16050529

763 27. Arnaud F, Caporale M, Varela M, Biek R, Chessa B, Alberti A, et al. A paradigm
764 for virus-host coevolution: sequential counter-adaptations between endogenous
765 and exogenous retroviruses. PLoS pathogens. 2007;3: e170.
766 doi:10.1371/journal.ppat.0030170

767 28. Zhang K, Kong H, Liu Y, Shang Y, Wu B, Liu X. Diagnosis and phylogenetic
768 analysis of ovine pulmonary adenocarcinoma in China. Virus Genes. 2014;48:
769 64–73. doi:10.1007/s11262-013-0988-x

770 29. Huang Q, Ye C, Chen T, Jiang J, Peng Y, Chen J, et al. EvaGreen-based real-
771 time PCR assay for sensitive detection of enzootic nasal tumor virus 2. Molecular
772 and Cellular Probes. 2019;44: 51–56. doi:10.1016/j.mcp.2019.02.003

773 30. Shi W, Jia S, Guan X, Yao X, Pan R, Huang X, et al. A survey of jaagsiekte sheep
774 retrovirus (JSRV) infection in sheep in the three northeastern provinces of China.
775 Arch Virol. 2021;166: 831–840. doi:10.1007/s00705-020-04919-6

776 31. Abass FA, Khudhair YI. Clinical, molecular, and pathological investigations of
777 ovine pulmonary adenocarcinoma in the middle of Iraq. Open Vet J. 2022;12:
778 264–272. doi:10.5455/OVJ.2022.v12.i2.15

779 32. Zhang X-L, Deng Y-P, Yang T, Li L-Y, Cheng T-Y, Liu G-H, et al. Metagenomics
780 of the midgut microbiome of Rhipicephalus microplus from China. Parasit
781 Vectors. 2022;15: 48. doi:10.1186/s13071-022-05161-6

782 33. Atim SA, Ashraf S, Niebel M, Ssekagiri A, Hardy MN, Shepherd JG, et al. Ticks;
783 a reservoir for virus emergence at the human-livestock interface in Uganda.
784 bioRxiv. 2023; 2023.03.10.532017. doi:10.1101/2023.03.10.532017

785 34. Zhang Y, Cheng T-Y, Liu G-H, Liu L, Duan D-Y. Metagenome reveals the midgut
786 microbial community of Haemaphysalis qinghaiensis ticks collected from yaks
787 and Tibetan sheep. Parasit Vectors. 2024;17: 370. doi:10.1186/s13071-024-
788 06442-y

789 35. Jamil A, Yu Z, Wang Y, Xin Q, Gao S, Abdul Wahab M, et al. Tick-borne
790 Rickettsia, Anaplasma, Theileria, and enzootic nasal tumor virus in ruminant,
791 PET, and poultry animals in Pakistan. Front Microbiol. 2024;15: 1359492.
792 doi:10.3389/fmicb.2024.1359492

36. Ndione MHD, Ndiaye EH, Dieng M, Diouf B, Sankhé S, Diallo D, et al. Mosquito-based detection of retroviruses and arboviruses in Senegal: expanding the scope of xenosurveillance. One Health Outlook. 2025;7: 32. doi:10.1186/s42522-025-00155-7

37. Zhou K, Zhang L, Li W, Feng Q, Zhao W, He W, et al. Metagenomic sequencing of epidemic pathogens in Ornithodoros lahorensis from southern Xinjiang. Medycyna Weterynaryjna. 2026;82: 135–141. doi:10.21521/mw.7113

38. Brait N, Hackl T, Morel C, Exbrayat A, Gutierrez S, Lequime S. A tale of caution: How endogenous viral elements affect virus discovery in transcriptomic data. Virus Evolution. 2024;10: vead088. doi:10.1093/ve/vead088

39. Katoh K, Standley DM. MAFFT Multiple Sequence Alignment Software Version 7: Improvements in Performance and Usability. Molecular Biology and Evolution. 2013;30: 772–780. doi:10.1093/molbev/mst010

40. Canty A, Ripley B, maintainer 1999--2022, support) author of parallel, fixes) ARB (minor bug. boot: Bootstrap Functions (Originally by Angelo Canty for S). 2024. Available: https://cran.r-project.org/web/packages/boot/index.html

41. Da Silva Teixeira MF, Lambert V, Mselli-Lakahl L, Chettab A, Chebloune Y, Mornex JF. Immortalization of caprine fibroblasts permissive for replication of small ruminant lentiviruses. Am J Vet Res. 1997;58: 579–584.

42. SCHERER WF, SYVERTON JT, GEY GO. Studies on the propagation in vitro of poliomyelitis viruses. IV. Viral multiplication in a stable strain of human malignant epithelial cells (strain HeLa) derived from an epidermoid carcinoma of the cervix. J Exp Med. 1953;97: 695–710. doi:10.1084/jem.97.5.695

43. Kent WJ. BLAT—The BLAST-Like Alignment Tool. Genome Res. 2002;12: 656–664. doi:10.1101/gr.229202

44. Salavati M, Caulton A, Clark R, Gazova I, Smith TPL, Worley KC, et al. Global Analysis of Transcription Start Sites in the New Ovine Reference Genome (Oar rambouillet v1.0). Front Genet. 2020;11: 580580. doi:10.3389/fgene.2020.580580

45. Davenport KM, Massa AT, Bhattarai S, McKay SD, Mousel MR, Herndon MK, et al. Characterizing Genetic Regulatory Elements in Ovine Tissues. Front Genet. 2021;12: 628849. doi:10.3389/fgene.2021.628849

46. Davenport KM, Bickhart DM, Worley K, Murali SC, Salavati M, Clark EL, et al. An improved ovine reference genome assembly to facilitate in-depth functional annotation of the sheep genome. GigaScience. 2022;11: giab096. doi:10.1093/gigascience/giab096

47. Karagianni AE, Vasoya D, Finlayson J, Martineau HM, Wood AR, Cousens C, et al. Transcriptional Response of Ovine Lung to Infection with Jaagsiekte Sheep Retrovirus. J Virol. 2019;93: e00876-19. doi:10.1128/JVI.00876-19

48. Bolger AM, Lohse M, Usadel B. Trimmomatic: a flexible trimmer for Illumina sequence data. Bioinformatics. 2014;30: 2114–2120. doi:10.1093/bioinformatics/btu170

49. Li H, Durbin R. Fast and accurate short read alignment with Burrows–Wheeler transform. Bioinformatics. 2009;25: 1754–1760. doi:10.1093/bioinformatics/btp324

50. Robinson JT, Thorvaldsdóttir H, Winckler W, Guttman M, Lander ES, Getz G, et al. Integrative genomics viewer. Nat Biotechnol. 2011;29: 24–26. doi:10.1038/nbt.1754

51. Nguyen L-T, Schmidt HA, von Haeseler A, Minh BQ. IQ-TREE: A Fast and Effective Stochastic Algorithm for Estimating Maximum-Likelihood Phylogenies. Molecular Biology and Evolution. 2015;32: 268–274. doi:10.1093/molbev/msu300

Legends Supporting information captions

S1 Table. Accession number list of all full-length and near full sequences of JSRV, ENTV-1, ENTV-2 and ERVs used in the study.

S2 Table. Description of the 286 JSRV and ENTV published primers used in the study.

The 'Publication specificity' column relies on the authors' statement of whether the primer pair was specific ("S") or not ("NS") for JSRV or ENTVs in the corresponding article(s). The 'Predicted XRV' column is based on *in silico* control of the specificity for XRV (Yes) or non-XRV (No). "ND" indicates that the XRV or ERV specificity could not be determined.

S3 Table. Sets of primers tested for XRV detection and PCR conditions.

S1 Fig. Characterisation of the k-mers used to detect ERV II.5 and JSRV reads.

The k-mers were identified from multiple alignments (MAFFT) of JSRV strains present in GenBank, whose exogenous nature was validated, and the copies of ERV II.5 Oa annotated in the ARS-UI_Ramb_v2.0 genome which contains the DR1 region (A), the DR3 region (B) or the DR4 region (C). Mismatches against the chosen k-mers are highlighted.

S2 Fig. Individual identity scores per XRV sequence. The individual identity scores for all the XRV sequences were calculated using a multiple alignment (MAFFT) of the XRV sequences against an ERV II.5 Oa consensus for JSRV (A) and ENTV-1 (B), and

869 against an ERV II.5 Ch consensus for ENTV-2 (C). The average identity percentage
870 was calculated using a 100-base pair window and plotted in steps of 10.

871 **S3 Fig. DR1-DR4 discriminating regions between endogenous retroviruses and**
872 **JSRV & ENTVs.** Viral genomic sequence of ERV II.5 Oa and Ch consensus
873 sequences [6] and JSRV clade I (FR2054; PP707050.1), clade II (FR989;
874 PP707047.1), ENTV-1 (FR4403, PP669280.1) and ENTV-2 (FR3824, PP669281.1)
875 were aligned using MAFFT. **A.** DR1 and **B**. DR2 in the *gag* gene. For DR2 the
876 percentage of each nucleotide (A,T,G,C) per position for all the II.5 copies in the Goat
877 (ARS1.2) and Sheep (ARS-UI_Ramb_v2.0) references was plotted in the deletion
878 area. **C.** DR3 in *env* and **D.** DR4 in U3. Only distinct nucleotides with the first sequence
879 of the alignment (ERV II.5 Oa) have been indicated, identical nucleotides are marked
880 by a dot. Numbering corresponds to the position on the alignment.

881 **S4 Fig. HERV-k sequence obtained with primer pair #4, supposedly specific of**
882 **ENTV-2 from genomic DNA of human HeLa cells.** Alignment (MAFFT) of the
883 sequence of PCR fragment #4 obtained by the Sanger method with the closest β-
884 HERV (HERVK-13) identified by BLAT.

885 **S5 Fig. Sequencing amplicons obtained from ovine IDO5 cells.** MAFFT alignment
886 of the amplicon sequence with ERV II.5 Oa consensus sequence. **A.** Primers set #3.
887 **B.** Primers set #4. **C.** Primers set #5. **D.** Primers set #6. **E.** Primers set #7. **F.** Primers
888 set #8. **G.** Primers set #14.

889 **S6 Fig. KT266728.1 Env sequence does not contain the oncogenic « YXXM »**
890 **motif.** The JSRV viral sequences KT266728.1, reported as the best match in [36], was
891 aligned (MAFFT) with the ERV II.5 Oa consensus sequence [6] as well as with JSRV
892 clade I (FR2054; PP707050.1) and clade II (FR989; PP707047.1) sequences. The

893 nucleotides encoding YXXM are not present in KT266728.1; this strain has a HKXM
894 predicted sequence that is common to ERV II.5.
895 **S7 Fig. Verification of metagenomic sequences identified as exogenous.** The
896 consensus sequence (TickP118) obtained from one tick metagenome from [33] and
897 the viral genomic sequence of ERV II.5 Oa and Ch consensus sequences [6] and
898 JSRV clade I (FR2054; PP707050.1), clade II (FR989; PP707047.1), ENTV-1
899 (FR4403, PP669280.1) and ENTV-2 (FR3824, PP669281.1) were aligned using
900 MAFFT in A. DR1, B. DR2 , C. DR3 and D. DR4. Only distinct nucleotides with the first
901 sequence of the alignment (ERV II.5 Ch) have been indicated, identical nucleotides
902 are marked by a dot. Numbering corresponds to the position on the alignment. Full-
903 length sequences of ENTV-2 and enENTV available on GenBank and the consensus
904 sequence obtained from one tick metagenome from [33] were used for phylogenetic
905 reconstructions. Maximum likelihood (ML) trees were reconstructed using PhyML **F.**
906 the 449-nt DR3 to DR4 region. Bootstrap values (1000 replicates) are expressed as a
907 percentage and indicated at the node level. To help the visualisation the tree was
908 rooted on the ERV branch. The scale bar indicates the number of substitutions per
909 site.
910
911

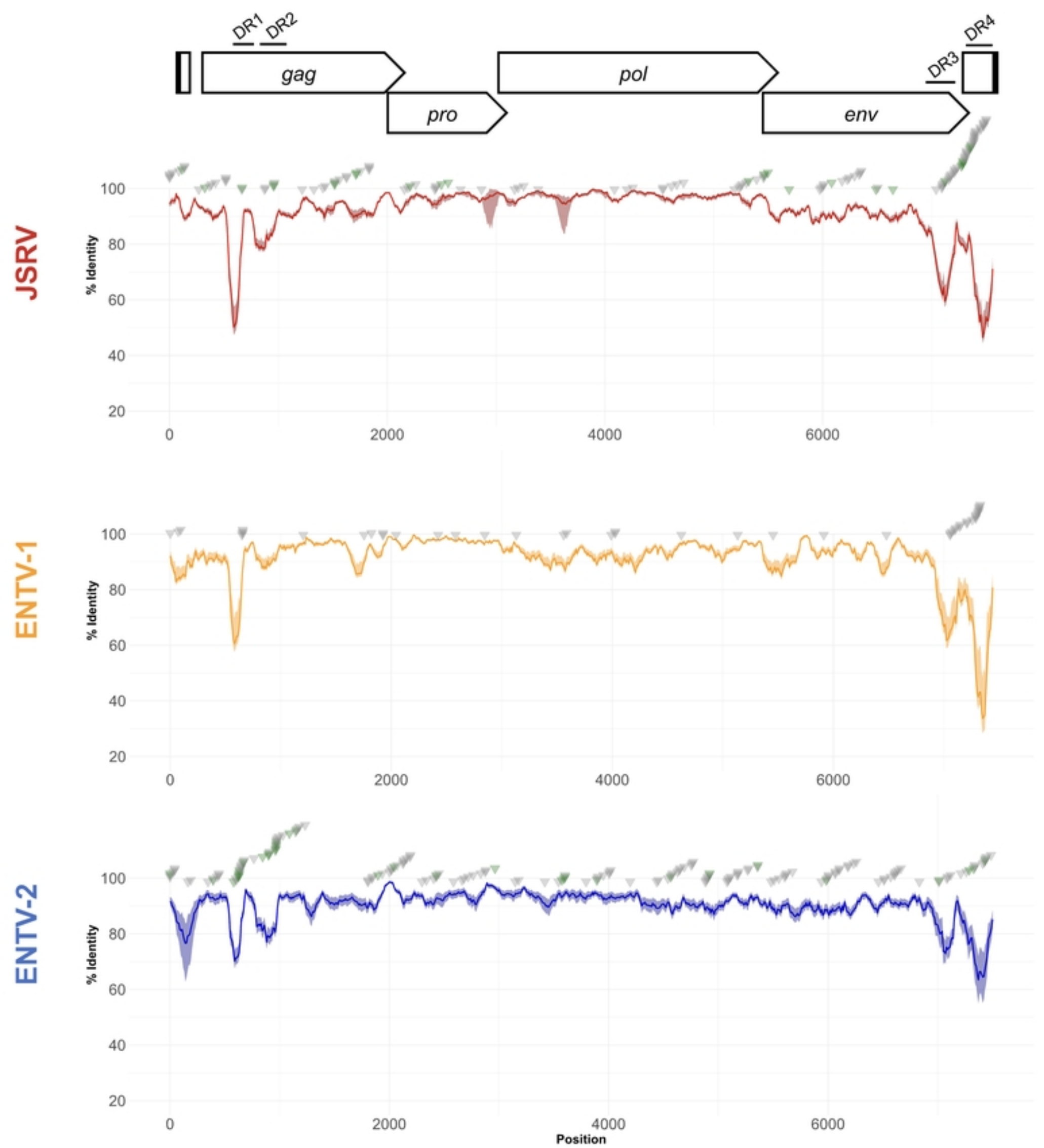

Figure 1

Figure 1

A. *pol*

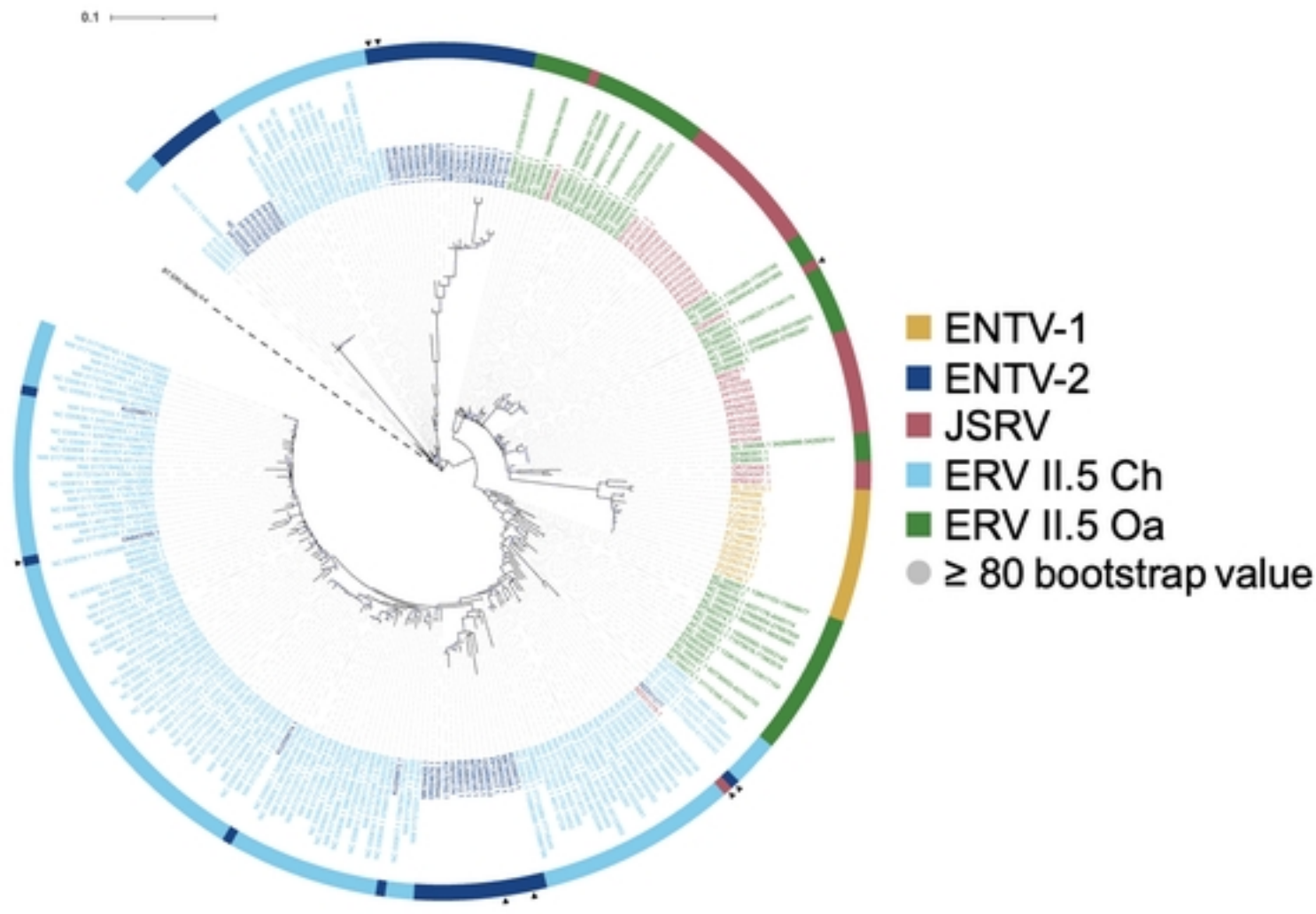

B. DR1 to DR2

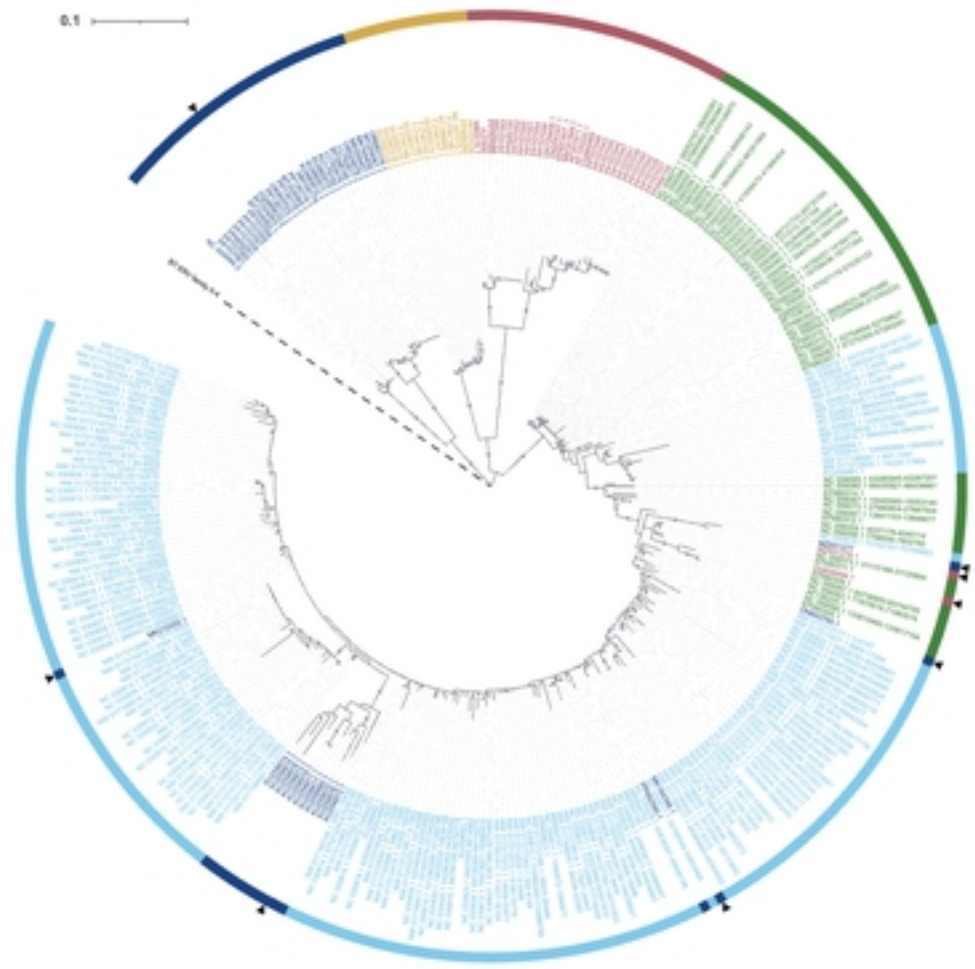

C. DR3 to DR4

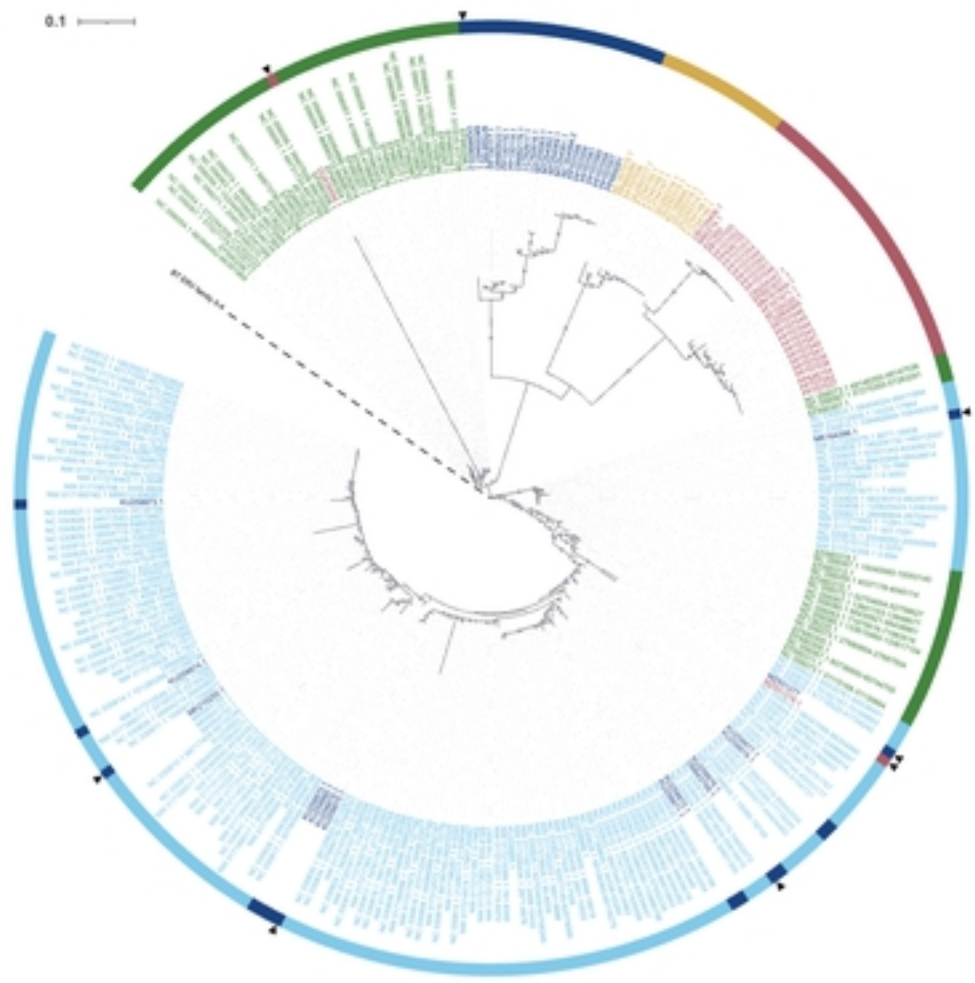

Figure 2

Figure 2

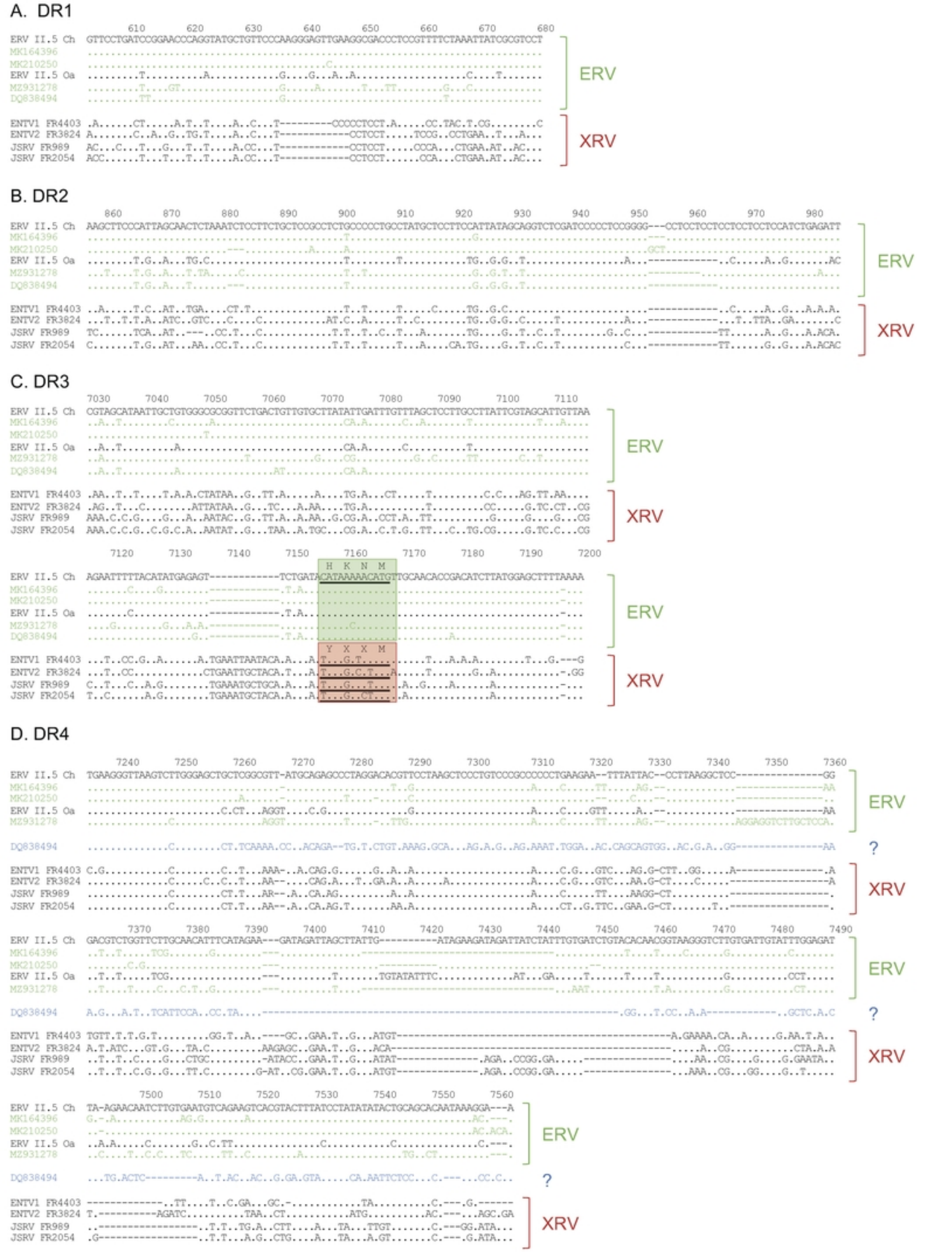

Figure 3

Figure 3

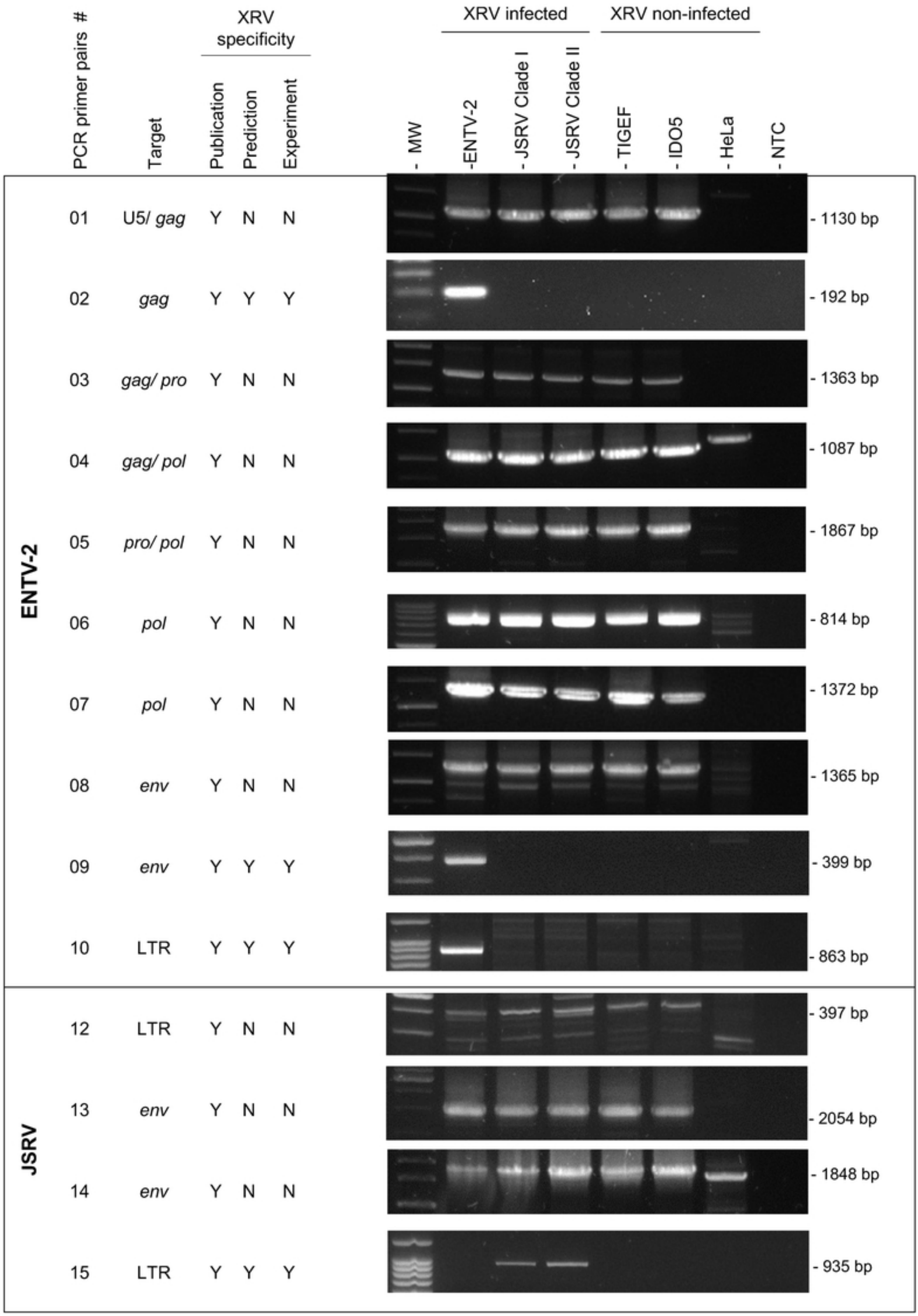

Figure 4

Figure 4

A. Alignment in the U5/gag DR1 region (amplicon PCR #01)

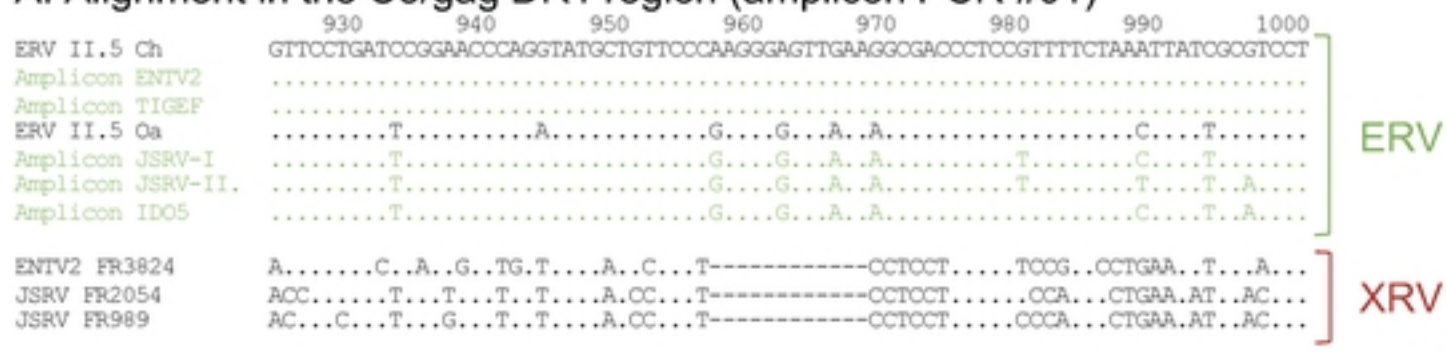

B. Alignment in the *env* DR3 region (amplicon PCR #13)

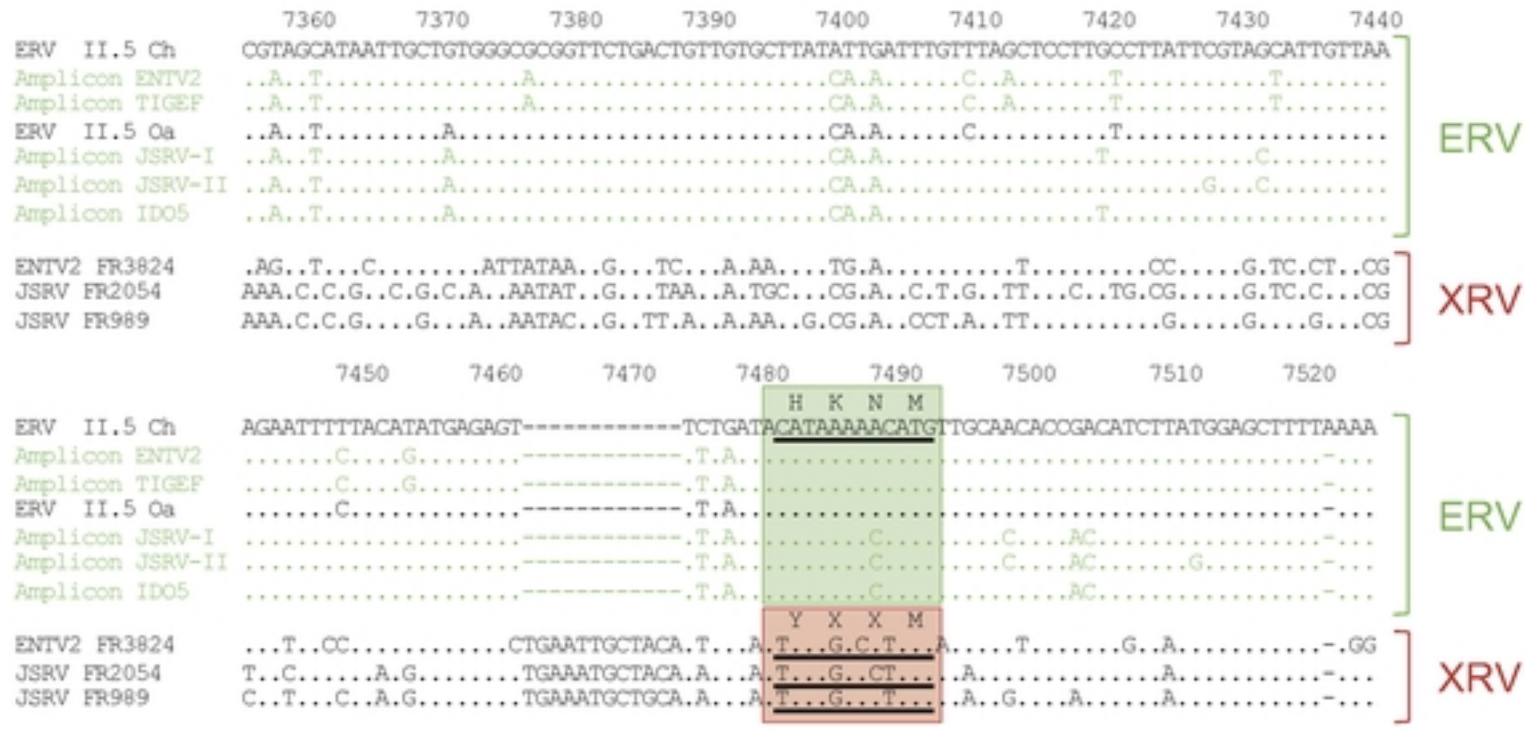

C. ENTV2 U5/*gag* (PCR #01)

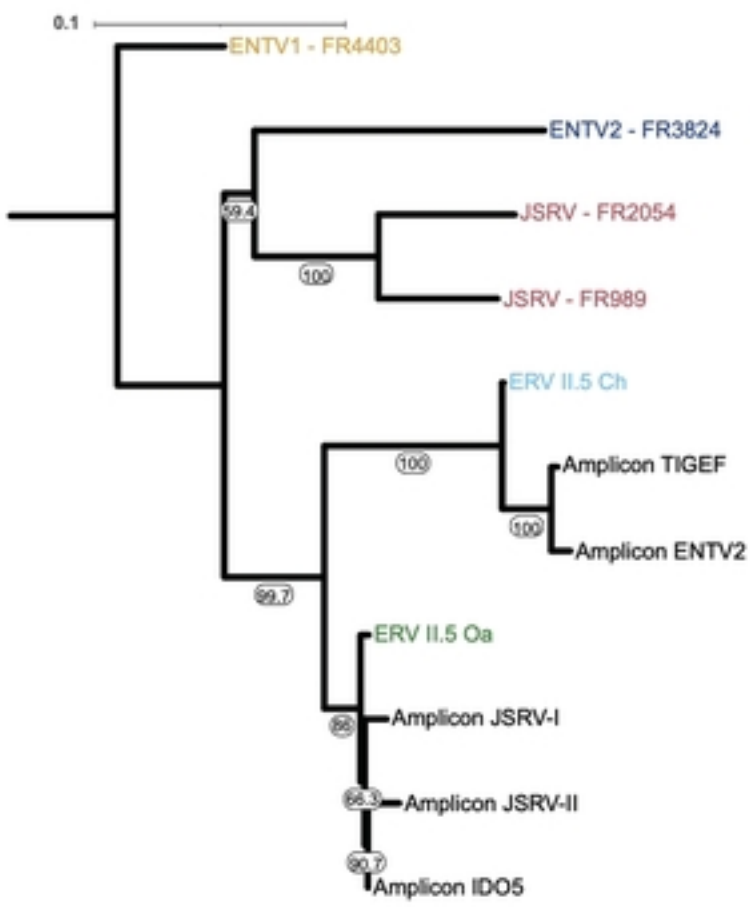

D. JSRV *env* (PCR #13)

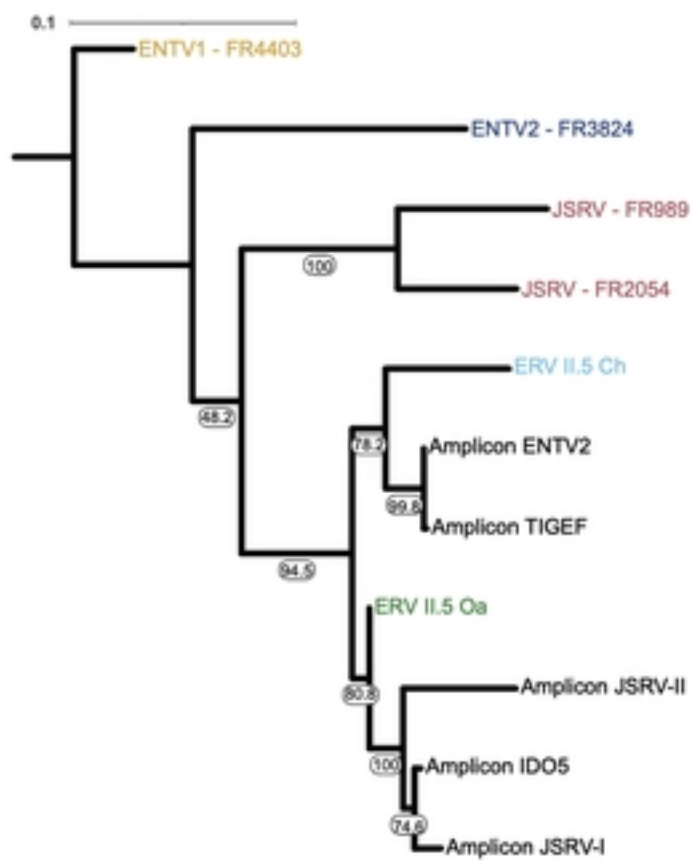

Figure 5

Figure 5

A. Localization of kmers

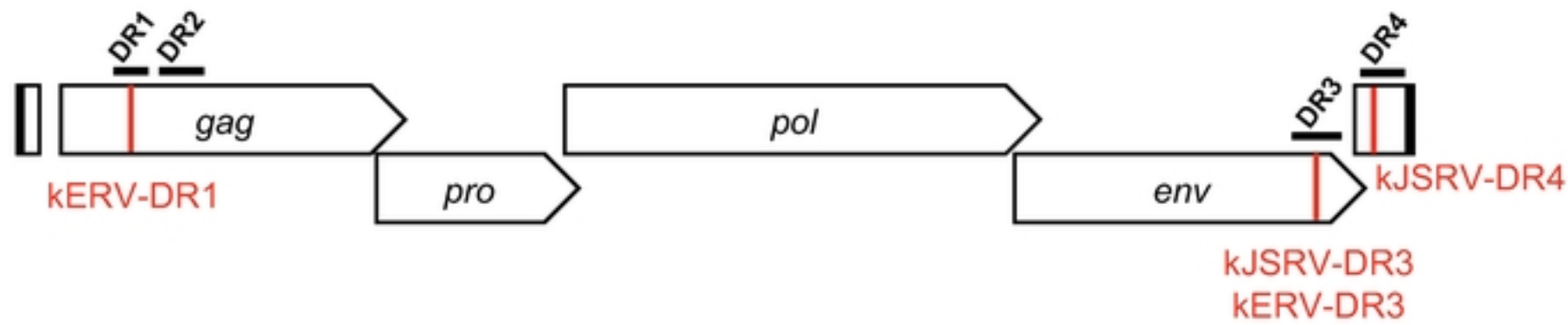

B. Expression of ERV II-5 in organs and tissues

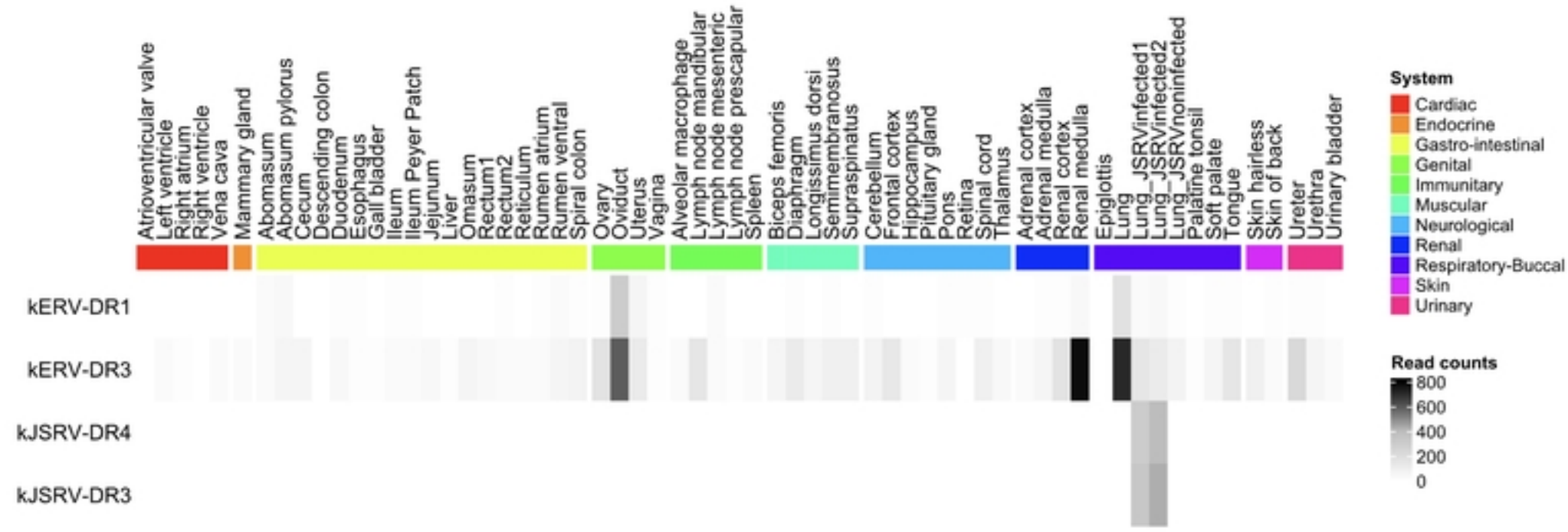

C. Mapping of selected reads on ERV II.5 Oa consensus sequence

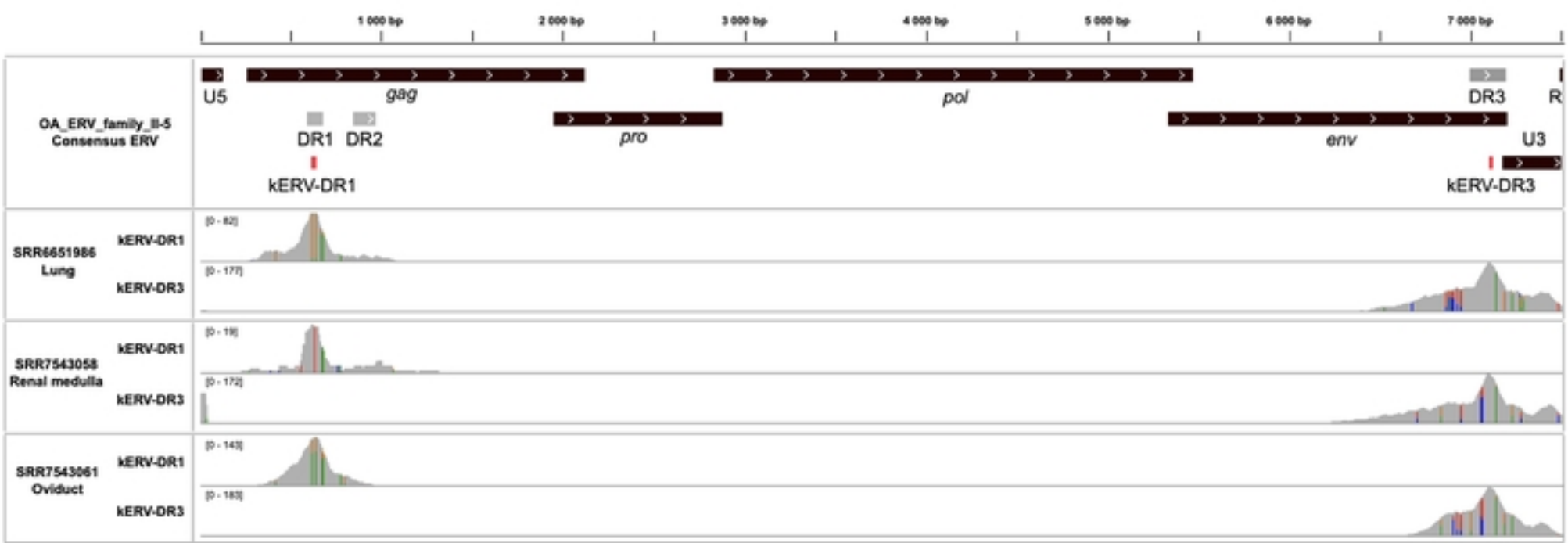

Figure 6

Figure 6

A. Primer specifcity

PCR primer pair #	Target	XRV specificity: Publication	Prediction	Experiment
16	*env*	Y	N	N
17	*U3/ R*	Y	N	N

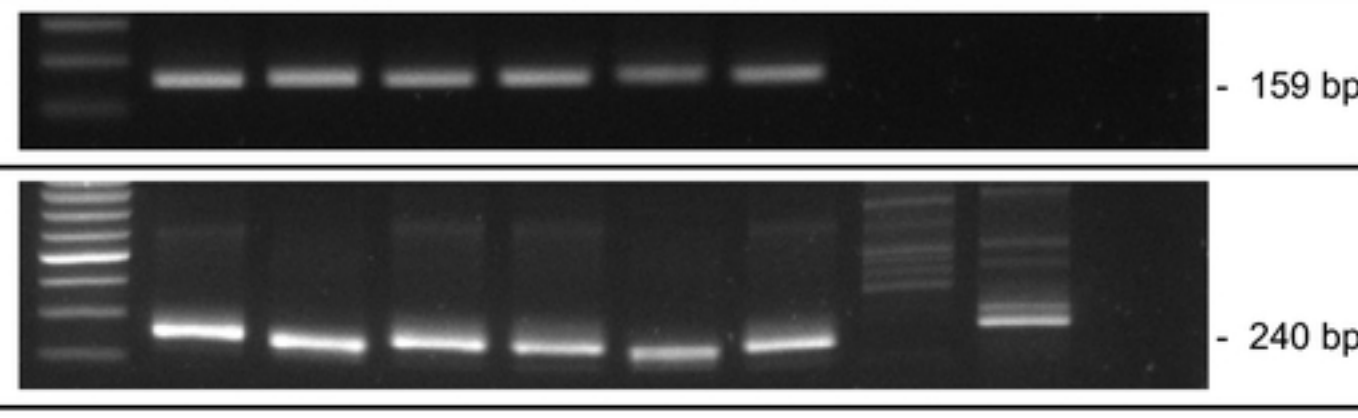

B. Alignment of the DR3 region (amplicon PCR #16)

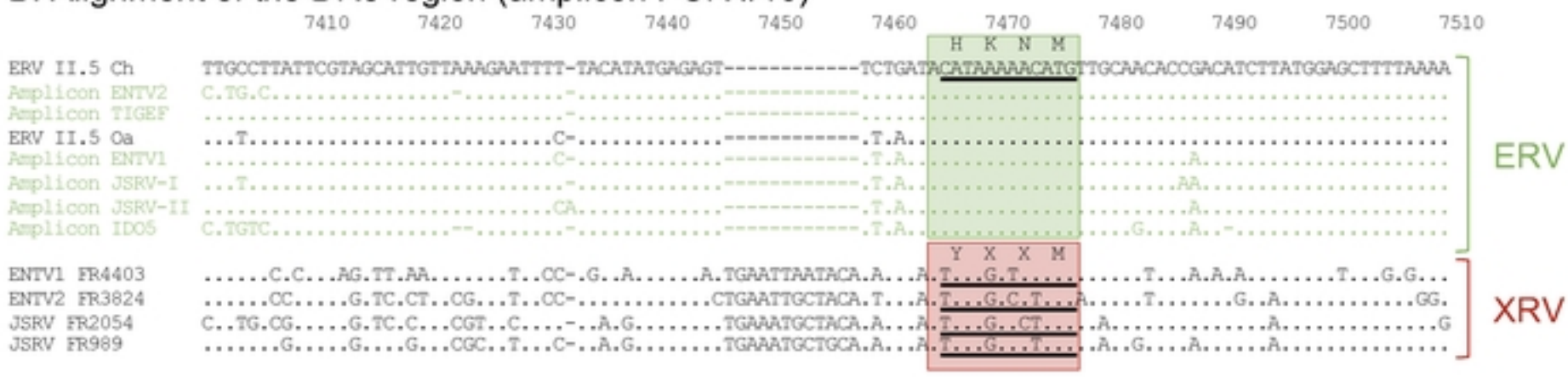

C. Alignment of the DR4 region (amplicon PCR #17)

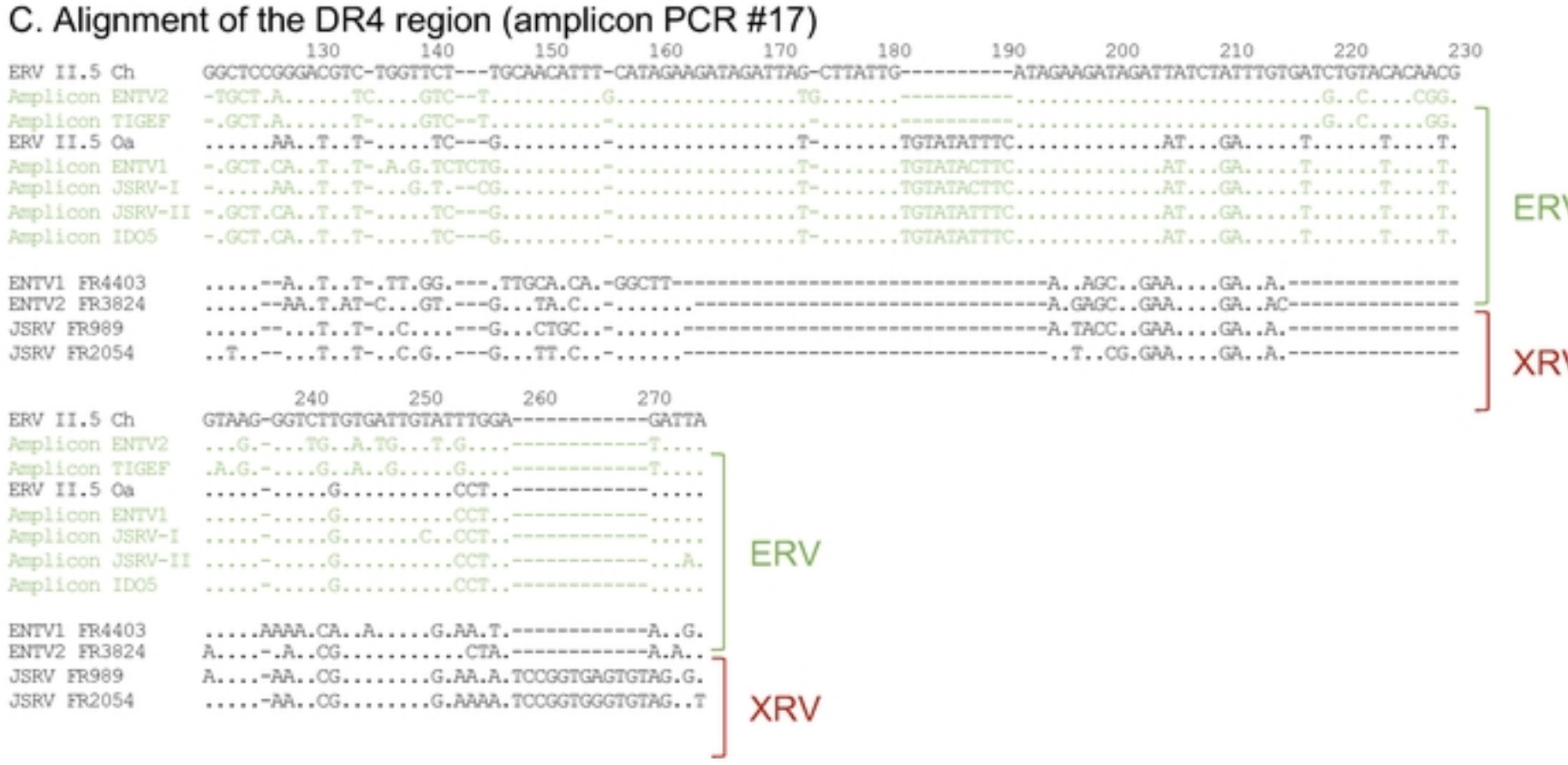

Figure 7

Figure 7

A. Alignment of OR991120 with reference sequences

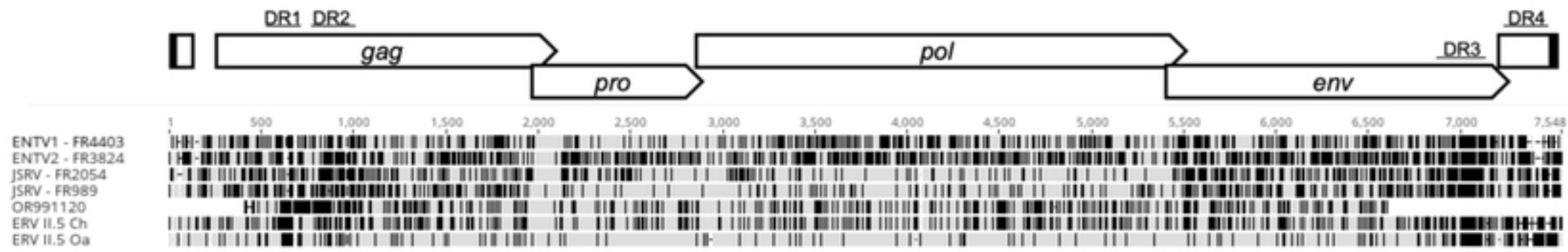

B. Primer specificity

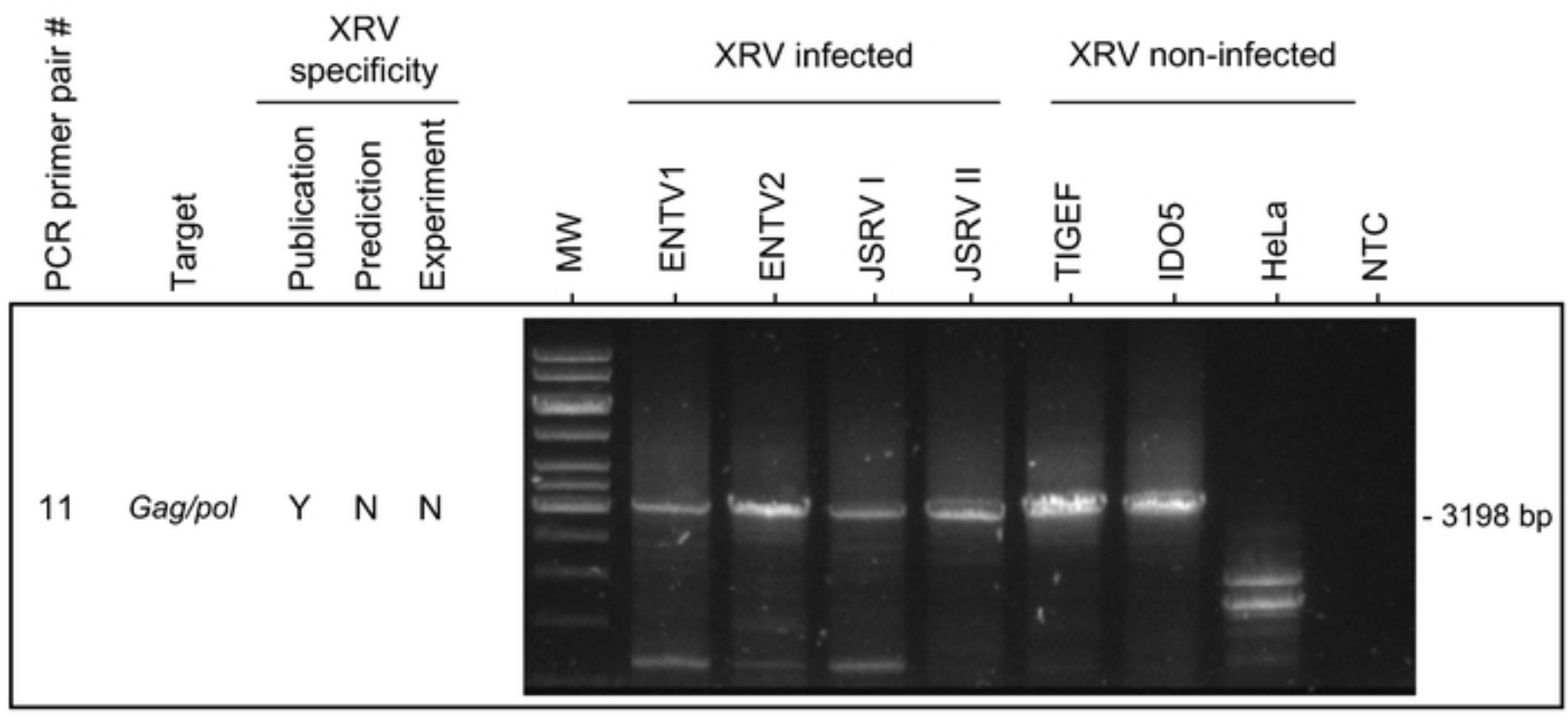

C. Alignment in the DR1 region (amplicon PCR #11)

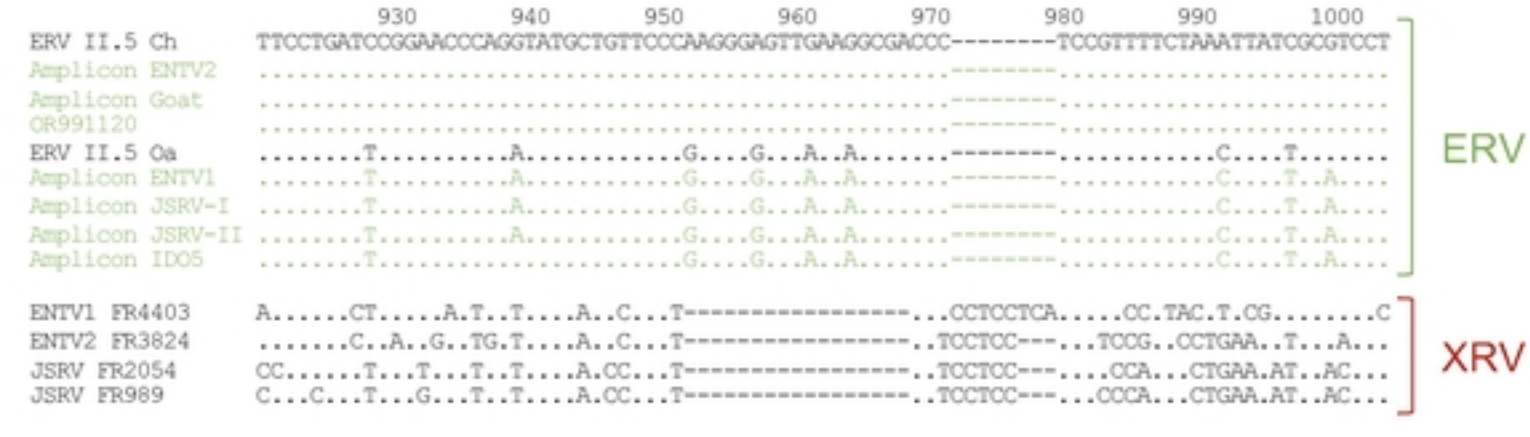

D. Alignment in the DR2 region (amplicon PCR #11)

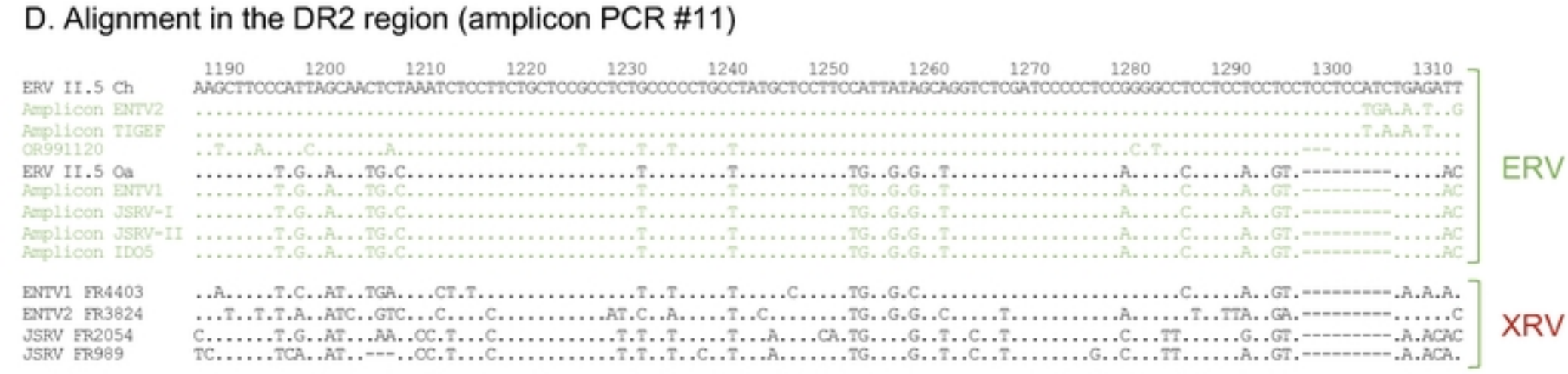

Figure 8

Figure 8